

**DEVELOPMENT OF MIDDLE JURASSIC MICROBIAL BUILDUPS
IN THE BIGHORN BASIN OF NORTHERN WYOMING**

A Thesis by
MANWIKA PLOYNOI

Bachelor of Science, Microbiology,
Chulalongkorn University, 2002

Submitted to the department of Liberal Arts and Sciences
and the faculty of the Graduate School of
Wichita State University
in partial fulfillment of
the requirements for the degree of
Master of Science

May 2007

**DEVELOPMENT OF MIDDLE JURASSIC MICROBIAL BUILDUPS
IN THE BIGHORN BASIN OF NORTHERN WYOMING**

I have examined the final copy of this thesis for form and content and recommend that it be accepted in partial fulfillment of the requirements for the degree of Master of Science with a major in Geology.

William C. Parcell, Thesis Committee Chair

We have read this Thesis
and recommend its acceptance:

Salvatore J. Mazzullo, Thesis Committee Member

Collette D. Burke, Thesis Committee Member

Jason W. Ferguson, Thesis Committee Member

ACKNOWLEDGEMENTS

I would like to thank my advisor, Dr. William C. Parcell for helping with support and financial assistance throughout the thesis from project conception through the writing process. Thanks to Jaci Venhaus, Monica Turner, and Andy Haner for their help during the summer 2005 field season. Thanks to thesis committee members Dr. Mazzullo, Dr. Burke and Dr. Ferguson. Thanks also to Wichita State University and Geology faculty for providing transportation to the study area. Luis Gonzalez of the W.M. Keck Environmental Laboratory of the University of Kansas was extremely helpful in preparing and running the carbon and oxygen stable isotopes. And also thanks to my parents for their support in everything.

ABSTRACT

This research examines the development of microbial buildups in the Middle Jurassic Lower Sundance Formation in the Bighorn Basin of northwestern Wyoming. Previous studies of Jurassic microbial research have focused on development along the Tethys Sea. This research examines buildups along the western side of the North America continent, in present day Wyoming. Microbial buildups were studied through outcrop measurements, hand sample and petrographic analysis. In addition, the stable carbon and oxygen isotopic composition were run to explain paleoclimate and chemical composition of seawater during the Middle Jurassic. The studied outcrop is located in northern Wyoming near Cody along the east side of Cedar Mountain. The microbial outcrop has an excellent semi-circular, exposure of microbial buildups at the location. The buildups are about 2.27 meters in height, 2.9 meters in width and 30 cm in thickness. The microbial buildups are composed of several thrombolitic heads.

The microbial buildups are associated with the Gypsum Spring and Lower Sundance Formation. The microbial units were deposited along a contact between these two Formations. The lithology of the Gypsum Spring is dominated by massive white gypsums at the lower unit and red shale at the upper unit. These deposited evaporites represent hypersaline condition with seasonally arid and warm climate over an extended period. The lithology of the Lower Sundance Formation is dominated by basal oolitic grainstone at the contact between itself and the Gypsum Spring Formation. The Lower Sundance Formation is also dominated by green shale and carbonate rocks with highly abundant in fossil especially ostracods, crinoids, and pelecypods. Based on petrographic analysis, the microbial buildups have thrombolitic or clotted characteristic features. Thrombolite structures are produced by sediment trapping, binding and/or precipitation as a result of the growth and metabolic activity of microorganisms, principally cyanobacteria. The thrombolite or bindstone is composed of highly clotted-looking algae such as *Girvanella* (Cyanobacteria), *Cayeuxia* (Chlorophyta), *Solenopora* (Rhodophyta) and other encrusting microorganisms such as foraminifera, ostracods, bryozoan, and cyanobacteria.

The isotopic composition values of belemnites can be used as a proxy for chemical composition of marine water because belemnites are believed to have not fractionated. As a result, belemnite calcite constitutes the best standard for the geochemistry of Jurassic seawater and provides a reasonable

approximation of sea water chemistry during deposition of a rock unit. The carbon isotopic values of belemnite from the Sundance Formation are 2.11 to 2.54 ‰, and oxygen isotopic values are -2.34 to -2.36‰. The carbon isotopic values of carbonate rock samples including microbial thrombolite from the Lower Sundance Formation range from 1.5 to 2.5 ‰, and an oxygen isotopic value range from -5.5 to -9 ‰. Overall, the isotopic values of carbonate rocks from the Lower Sundance Formation of the study section are more negative than the standard for seawater as represented by the belemnite isotopic values. The result of the entire stratigraphic column has been altered post-depositionally. Negative values suggest that rocks have been diagenetically altered by meteoric water since deposition during the Jurassic. As a result, carbon and oxygen isotopes can not be used to determine original sea water chemistry. However isotopic composition values from the belemnite can be used to determine paleotemperature. The paleotemperature of the Middle Jurassic (Late Bathonian to Early Callovian) seawater based on the belemnite samples from Wyoming is calculated to about 15-17°C.

TABLE OF CONTENTS

Chapter	Page
I. INTRODUCTION	1
A. Purpose and Scope of Study	1
B. Location and Geologic Setting	2
C. Paleogeography and Paleoclimate	2
D. Jurassic Western Interior Seaway	5
E. Microbialite Classification	9
II. METHODOLOGY	11
Methods and Procedures	11
III. PREVIOUS STRATIGRAPHIC INVESTIGATIONS	14
A. General Stratigraphy of the Bighorn Basin.....	14
B. Middle Jurassic Stratigraphy of Northwestern Wyoming.....	19
1) Gypsum Spring Formation	21
2) Sundance Formation	22
IV. THE FIELD/OUTCROP LITHOLOGY	24
A. Stratigraphy of Gypsum Spring Formation	30
1) Gypsum Facies	30
2) Dolomite Facies	30
3) Reddish-Brown Shale Facies.....	33
4) Gray-Green Shale Facies	33
5) Lime Mudstone Facies	33
6) Wackestone and Packstone Facies	33
B. Lithology of Lower Sundance Formation	34
1) Olive-Brown Shale Facies	34
2) Gray-Green Shale Facies	34
3) Lime Mudstone Facies	34
4) Wackestone and Packstone Facies	34

5) Grainstone Facies	38
6) Microbial Thrombolite Facies	38
C. Stratigraphic Analysis	41
1) Cross-Section Correlation	41
2) Lithology and Climatic Discussions.....	43
V. PETROGRAPHIC ANALYSIS	45
A. Microfacies of Lower Sundance Formation	45
1) Mudstone Microfacies	45
2) Wackestone and Packstone Microfacies	47
3) Grainstone Microfacies	52
4) Microbial Thrombolite Microfacies.....	52
B. Discussion of Allochems and Fossils	57
1) Ostracods	57
2) Ooids	58
3) Algae	58
4) Cyanobacteria	59
VI. ISOTOPIC ANALYSIS	60
A. Results of Carbon and Oxygen Stable Isotope	65
B. Climate Interpretation	71
VII. CONCLUSIONS.....	72
REFERENCES	73
APPENDICES	78

LIST OF TABLES

Table		Page
1	Dimensions of microbial buildups	29
2	Stable isotopic composition values of carbon and oxygen	63
3	Rock sample descriptions	81
4	Petrographic analysis	84

LIST OF FIGURES

Figure		Page
1	Geological map of the Bighorn Basin Region	3
2	Middle Jurassic paleolatitude on the western of North America	4
3	Western Interior seaway during the Middle Jurassic period	6
4	Middle Jurassic (Bajocian-Early Callovian) paleogeography	7
5	Isotopic method diagram	13
6	General stratigraphy of sedimentary deposits in Bighorn Basin	15
7	Stratigraphic relationship of sedimentary deposits of Middle Jurassic in the Bighorn Basin	20
8	Location of study area in Park County, Wyoming	25
9	The studied microbial outcrop lies along a horizon at the contact between the Gypsum Spring and Lower Sundance Formation	26
10	The studied microbial outcrop	27
11	Top view of microbial outcrop including scale in centimeter	28
12	The location of sections near Cody from Middle Jurassic in the Bighorn Basin	31
13	Stratigraphy of the Middle Jurassic Gypsum Spring and Lower Sundance Formation, east of Cedar Mountain outcrop, WY	32
14	Facies 1: olive-brown shale lithology (ECM MP2) from Lower Sundance Formation at east of Cedar Mountain	35
15	Facies 3: lime mudstone lithology (ECM MP6, ECM MP9)	36
16	Facies 4: wackestone and packstone lithology (ECM MP1, ECM MP2, ECM MP 5, and ECM MP 7)	37
17	Facies 5: grainstone lithology (ECM MP3) from Lower Sundance Formation at east of Cedar Mountain	39
18	Facies 6: microbial thrombolite lithology (ECM S1, S2, S3, S4, and S5)	40
19	Stratigraphic cross-sections from north to south across Cody area	42
20	Mudstone microfacies (part I) include ECM MP6 and ECM MP8	46

21	Mudstone microfacies (part II) include ECM MP9	48
22	Packstone microfacies (part I: ECM MP1) from Lower Sundance Formation at east of Cedar Mountain	49
23	Packstone microfacies (part II: ECM MP2) from Lower Sundance Formation	50
24	Wackestone and Packstone microfacies (part III: ECM MP5 and ECM MP7)	51
25	Grainstone microfacies (ECM MP3) from Lower Sundance Formation at east of Cedar Mountain	53
26	Microbial thrombolite microfacies (part I) from Lower Sundance Formation at east of Cedar Mountain	54
27	Microbial thrombolite microfacies (part II) from Lower Sundance Formation	56
28	Rock samples for isotopic analysis (ECM MP1 to ECM MP9)	61
29	Rock samples for isotopic analysis (ECM S1 to ECM S5)	62
30	Carbon and oxygen isotopic values of Middle Jurassic in study area, WY	66
31	Carbon and oxygen isotopic composition curve	67
32	Carbon and oxygen isotope values of Oxfordian and Kimmeridgian reefs from Europe	70

CHAPTER I

INTRODUCTION

A. Purpose and Scope of Study

The Jurassic Period was an important time of extensive reef development and there have been many efforts to try to identify the local, regional and global controls on Jurassic reef growth (Leinfelder, 1993; Parcell, 2003). Jurassic reefs were often completely different in composition and biota to modern reefs. For example, soft sponges are particularly important in modern reefs but not in the Jurassic Period. In contrast, siliceous and calcareous sponges were more important in the Jurassic. This was partially due to regional and global environmental conditions different to those of our modern world. Such different reefs were nevertheless well adapted to their environments and hence may be used as monitors for paleo-environmental changes (Leinfelder, 1994). Varying biologic composition of these reefs may represent changing global, regional or local environmental changes. Jurassic reefs are also of increasing interest as petroleum reservoirs in places such as the Gulf Coast, U.S.A., offshore Northern Canada, and the former Soviet republics of Kazakhstan and Turkmenistan. As these reefs are commonly porous and were originally rich in organic matter, they are likely places for oil to generate and accumulate.

This study examines the Middle Jurassic microbial buildups from the western margin of the Bighorn Basin of north-central Wyoming using field descriptions, petrographic examination and stable isotopic analyses. These Middle Jurassic microbial buildups in Wyoming are of interest because these reefs exhibit a significant succession of well-exposed shallow water buildups. Furthermore, these buildups are among the earliest known occurrence of Jurassic microbial reefs in North America (Parcell and Williams, 2004, Dromart, personal communication, 2004). In addition, few microbial reefs of this age have been identified and examined from western North America. Results from this study are compared to well-studied Upper Jurassic microbial buildups of Europe.

B. Location and Geologic Setting

The Bighorn Basin is located in north-central Wyoming and south-central Montana. The section of interest occurs within the marine Jurassic units located in the Bighorn Basin of northwestern Wyoming. The Bighorn Basin is both a topographic and structural basin that is bound on the east by the Big Horn Mountains, on the south by the Owl Creek Mountains, and on the west by the Absaroka Plateau and Beartooth Mountains. The basin is constricted to the north by the Beartooth and Pryor Mountains and continues into Montana where it partially merges with the Crazy Mountain syncline across the Nye-Bowler lineament (Halverson, 1964). The Bighorn Basin is characterized by an asymmetrical structural depression with a sinuous northwest-trending axis (Samuelson, 1974), (Figure 1).

During the earliest Jurassic, North America was still part of the supercontinent Pangaea. As Pangaea continued its break up during the Jurassic, deposition in the western part of North America was influenced by the motion of the Farallon plate which resulted in a complex active margin developed along the western edge of North America (Johnson, 1991). During the Middle Jurassic, the Bighorn Basin was part of the Wyoming-Montana Shelf. Many of tectonic features controlled the seaway's configuration on this shelf (Peterson, 1957). These features include broad gentle uplifts such as the Belt Island, the Uncompahgre Uplift and the Sheridan Arch (Imlay, 1980). In addition to these positive areas, there were several large depressions and troughs such as the Williston Basin, the Twin Creek Trough, and the Harding Trough (Imlay, 1980).

C. Paleogeography and Paleoclimate

From the Triassic to Jurassic, the central and southern part of the Western Interior of the United States was located between 5° and 25° north latitude (Kocurek and Dott, 1983). During the Jurassic, the North American plate drifted northward with some clockwise rotation. During the Middle Jurassic (Bajocian to Callovian), the Wyoming region occupied a northern paleolatitude between 20° and 25° (Kocurek and Dott, 1983) (Figure 2).

The global mean temperature during the Mesozoic was perhaps as much as 10°C (18°F) higher than today (Kocurek and Dott, 1983). The breakup of Pangaea during the Late Triassic caused the global temperature gradient to increase. Wicander and Monroe (2004) propose that the steeper global

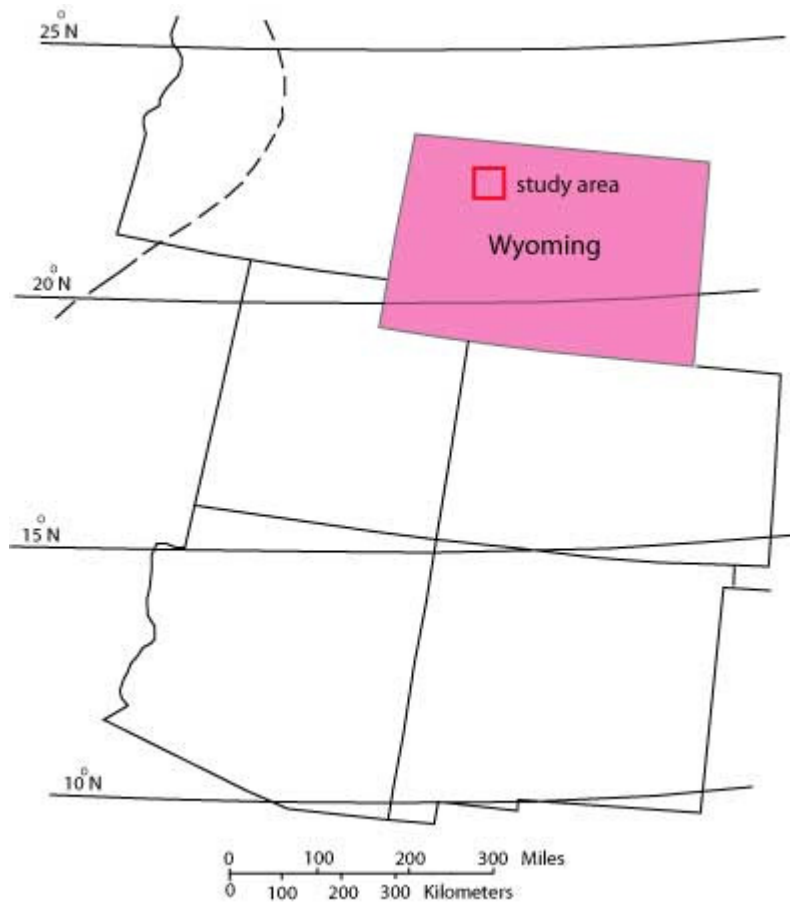


Figure 2: Middle Jurassic paleolatitude on the western of North America
(Modified from Kocurek and Dott, 1983)

temperature gradient greatly accelerated during Mesozoic because of a decrease in temperature in the high latitudes and changing positions of the continents, oceanic and atmospheric circulation patterns. Hallam (1975) suggests that the Jurassic climate was more equable than today's climate wherein the Earth had no polar ice caps. Warm, arid climatic conditions predominated in western North America, including Utah, Wyoming and South Dakota, and deposition was dominated by evaporite deposits.

The distribution and thickness of carbonate deposits have been used as evidence for a warm climate (Hallam, 1975). Likewise widespread reef development has also been used as an indicator for warm climates. According to Wells (1967), significant reef development only takes place above 18°C. Therefore coral reefs are confined today to the tropical-subtropical zone, from about 30°N to 30°S (Hallam, 1975).

D. Jurassic Western Interior Seaway

Hallam (1975) described the Jurassic Sea of the Western Interior as "occupying, to an extent varying over time, part or all of Montana, Wyoming, North and South Dakota, Idaho, Utah, Colorado and New Mexico" (Figure 3, and 4). The Interior Sea transgressed the study area several times during the Jurassic. The first marine transgression occurred during the Early Jurassic (Sinemurian) age, and is recorded in dark, phosphatic shales of the Fernie Group of southeastern British Columbia, northwestern Montana and eastern Oregon (Hallam, 1975). While this marine transgression is recorded along the western margin of the United States and in the Western Interior of Canada, there are no marine deposits of this age in the Bighorn Basin. Instead the Early Jurassic is represented by either nonmarine deposits or unconformities (J-1 unconformity of Piperigos and O'Sullivan, 1978). The J-1 unconformity is expressed by erosion of the Triassic Chugwater Group during the Latest Triassic and Earliest Jurassic (Johnson, 1991).

The second marine transgression (Early Bajocian) is recorded in the Bighorn Basin (Hallam, 1975; Imlay, 1980). The Bajocian Sea entered the North American continent from the north and west and extended as far south as northwestern Arizona and east across Wyoming into the Dakotas almost reaching Minnesota. These marine deposits can be identified by ammonites such as *Stephanoceras* and

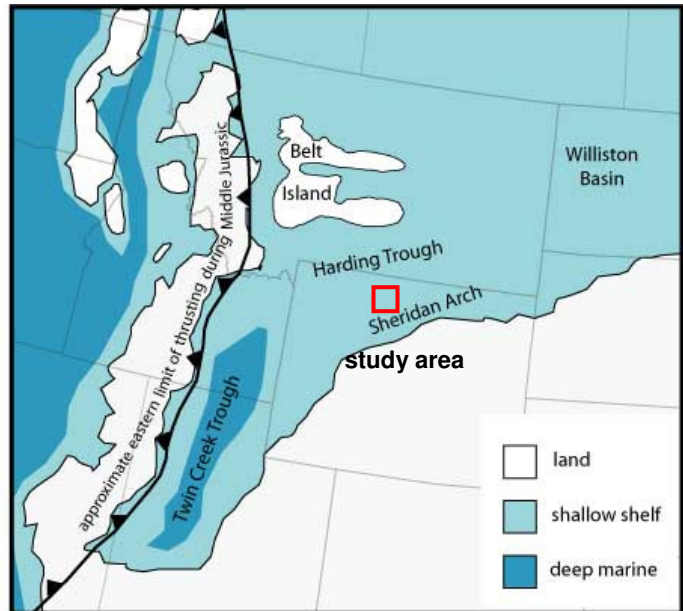
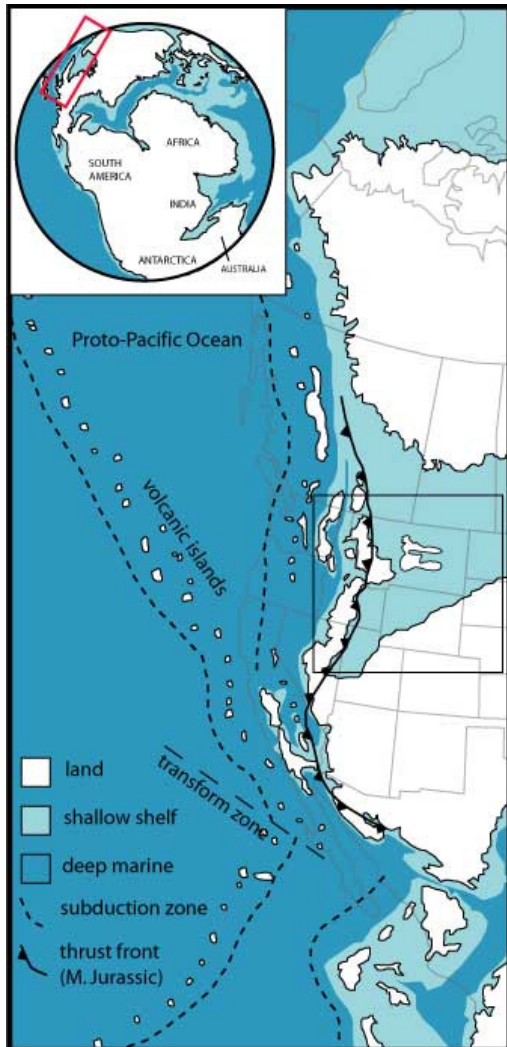


Figure 3: Western Interior Seaway during the Middle Jurassic Period (modified from Parcell, 2002)

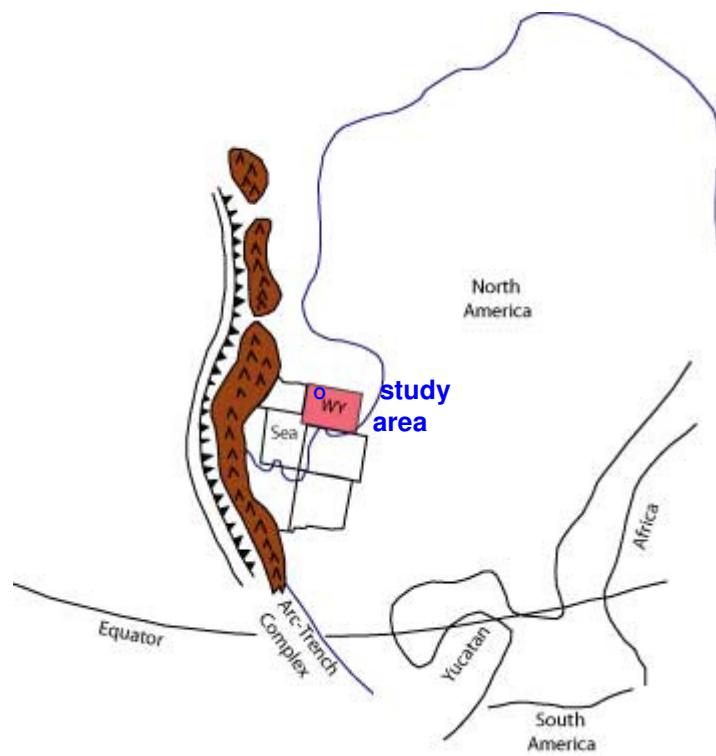


Figure 4: Middle Jurassic (Bajocian-Early Callovian) paleogeography. This figure represents the seaway that invaded western North America. (Modified from Kocurek and Dott, 1983)

Stemmatoceras (Hallam, 1975; Imlay, 1952a, and 1980). This second transgression is known as the Gypsum Spring Sea. The Gypsum Spring Sea was very shallow with hypersaline conditions predominating on the east side of the Interior seaway (Johnson, 1991). Sediments in Wyoming that were deposited in the Bajocian Sea are named the Gypsum Spring Formation (Imlay, 1980). After the Bajocian Sea retreated in the early to middle stages of Middle Bajocian, a period of erosion began throughout the Western Interior that is recognized today as the J-2 unconformity (Imlay, 1980; Hallam, 1988).

A third marine invasion, known as the Sundance Sea, occurred in the Late Bathonian to Early Callovian and extended inland further than the previous transgressions (Hallam, 1975; Johnson, 1991). This marine transgression is marked by a basal shallow-water calcareous oolite and sandstone overlain by shales with abundant *Gryphaea nebrascensis* (Hallam, 1975). Ammonites in this sequence include *Arctocephalites* (*Paracephalites*); *Arcticoceras* (*Warrenoceras*); *Kepplerites* and *Cadoceras* (Hallam, 1975). Retreat of this sea from the eastern side of the middle Western Interior during the late Middle Jurassic resulted in a local discontinuous unconformity (J-3) (Johnson, 1991).

The fourth and most extensive marine transgression or Pine Butte Sea occurred in the late Middle Jurassic (Callovian) (Hallam, 1975, Johnson, 1991). This rapid marine transgression completely submerged paleohighs, including Belt Island in central Montana, for the first time and extended far to the south and southeast. This sequence of units deposited during this transgression is dated as Early Oxfordian by the occurrence of ammonites *Quenstedtoceras* and *Cardioceras* (Hallam, 1975). The regression of this sea developed a regional unconformity (J-4) throughout much of the seaway (Johnson, 1991). The greatest erosion occurred in central and northwestern Montana in the Belt Island area (Imlay, 1980).

The fifth marine invasion of the Middle Western Interior, referred to as the Late Sundance Sea, began at the close of the Middle Jurassic when marine waters from the west spread over a central Montana and the Williston Basin area (Imlay, 1980; Johnson, 1991). Later in the Oxfordian, the sea regressed and is marked by a local and somewhat discontinuous unconformity (J-5) (Johnson, 1991). A final rapid transgression followed, which represents the sixth and final marine invasion. Johnson (1991)

recognized this deposition as the Windy Hill Sea. After the retreat of this sea, marine water had completely withdrawn from the middle Western Interior which ended the history of the Jurassic Western Interior Seaway (Johnson, 1991).

E. Microbialite Classification

Many terms have been used to describe rocks and sediments composed of microorganisms such as microbialite, microbolite, microbial crusts, microbial buildups and microbial mounds. They are interpreted as organosedimentary deposits resulting from microbial activity, mainly built by microbes, particularly cyanobacteria and other bacteria, such as photosynthetic and/or anaerobic bacteria, but commonly including other encrusting organisms such as algae and foraminifera (Leinfelder, 1993; Leinfelder et al., 2002). Microbes are abundant and widespread both in carbonate and siliciclastic sediments. Microbial films can stabilize loose sediment and provide for mineral nucleation. Therefore, microbes modify and create sediments (Mancini, et al. 2004). In addition, microbes can help protect sediment from erosion by coatings on sediment surface.

Development of microbial classification

Aitken (1967) proposed the term “cryptalgal structures for thrombolites which lack lamination and are characterized by a macroscopic clotted fabric”. Kennard and James (1986) proposed two distinct types of microbial (cryptalgal) structures which are thrombolites and stromatolites. They describe thrombolites as mesoscopic clotted fabric and stromatolites with laminated internal fabric. They also described thrombolitic clotted fabric is a primary microbial feature and not a disrupted or modified laminated fabric. They interpreted the individual mesoscopic clots, or mesoclots, within thrombolites as “discrete colonies or growth forms of calcified, internally poorly differentiated and coccoid-dominated microbial communities”. According to Leinfelder (1993), the basic types of microbial crusts have been described by their fabric. The fabric ranges from dense to peloidal to mostly clotted thrombolitic. Boggs (2000) suggested that microbial mounds are built by stromatolites, thrombolites and calcimicrobes (microbes capable of mediating carbonate precipitation). According to Burne and Moore (1987), microbialites are “organosedimentary deposits formed from interaction between benthic microbial communities (BMCs) and detrital or chemical sediments”. They suggested various processes involved in

the formation of calcareous microbialites, including the trapping and binding of detrital sediment (forming microbial boundstones), inorganic calcification (forming microbial tufa), and biologically influenced calcification (forming microbial framestones).

Thrombolitic crusts can develop in the settings of varying bathymetry, water-energy, salinity and oxygen/nutrient concentrations. Microbial crusts can include additional micro-encrusters of variable abundance and diversity (Leinfelder, 1993). The distribution of micro-encrusters has proven to be a useful tool for the estimation of bathymetry (Leinfelder et al. 1993b). The major prerequisite for thrombolite reef growth is a very low to zero sedimentation rates which allow the organisms to grow on top of sediments. Oxygen fluctuation is another factor that control the type of organisms contained in the reefs.

CHAPTER II

METHODOLOGY

Methods and Procedures

This study examined the development of the Middle Jurassic microbial buildups in three methodological phases. The first phase involved field measurements of the outcrop along the east side of Cedar Mountains of Bighorn Basin in Park County, northwestern Wyoming in order to identify the location of the microbial buildups in the outcrop. The focus of this phase was to perform stratigraphic measurements and collect field samples for petrographic and isotopic analysis. The information recorded from the outcrop location included measurement of stratigraphic section from the Gypsum Spring Formation at the base to the Sundance Formation at the top. A hand lens was used to describe and identify the texture, mineralogy and organisms contained in the stratigraphic section. Dunham's (1962) classification of carbonates and Munsell's soil color charts (2000) were used to describe textures and colors characteristic of soils, sediments, and most rocks in the field.

Phase two of the project involved petrographic analysis. Rock samples were collected from the microbial buildups themselves and from the formation immediately beneath these microbial buildups to make a thin section. Samples of individual heads were randomly chosen across the entire microbial buildup section in order to compare the results with each other. Thin sections were made from fourteen selected rock samples: 9 thin sections came from beds beneath the microbial mounds (MP1 to MP9); 5 thin sections came from individual heads of the microbial mounds (S1 to S5). These thin sections were all stained by alizarin acid, impregnated with blue epoxy and studied under binocular and polarizing microscopes to examine sedimentary texture, fossil assemblage, and mineral composition. This phase was emphasized to study and identify the organisms and micro-organisms such as algae, cyanobacteria, ostracods, and others. The classification of lithology and texture of the entire thin section is also based on Dunham's classification (1962). Thin section analysis provides more information about the organisms which is used to support the interpretation of the isotopic analysis of these microbial buildups.

Isotopic analysis is the final phase of the project. The purpose of this phase is to study the paleoclimate such as paleotemperature and composition of sea water during the Middle Jurassic. The stable isotopes of oxygen and carbon were taken from the bulk rocks contained in the stratigraphic column of Middle Jurassic Lower Sundance Formation. In order to measure the isotopic composition of the carbonate mud, the rocks were carefully selected and sampled in the zones where grains were scarce and bioturbation was minimal. Rock powder samples were analyzed for carbon and oxygen isotopic composition at the W.M. Keck Environmental Laboratory of the University of Kansas. Rock powder samples were taken from 23 cut and polished rock specimens and dried in an oven at 200°C for about an hour then all samples were weighed out to 30-50 µg after cooling.

Carbonate $\delta^{13}\text{C}$ and $\delta^{18}\text{O}$ values were measured in a Thermo Finnigan MAT 253 mass spectrometer. NBS-18 and NBS-19 were used as a standard for calibration in this stable isotope analysis and PDB was used as a reference. The tiny grains of each sample were put into the KPESIL KIEL device which was used to prepare carbonate samples to be run in the mass spectrometer machine (Figure 5). Phosphoric acid was added to each sample and gases were released into the GasBench II that line above the KIEL device. These gases passed through the magnet of MAT 253 which separates each isotope at different distances.

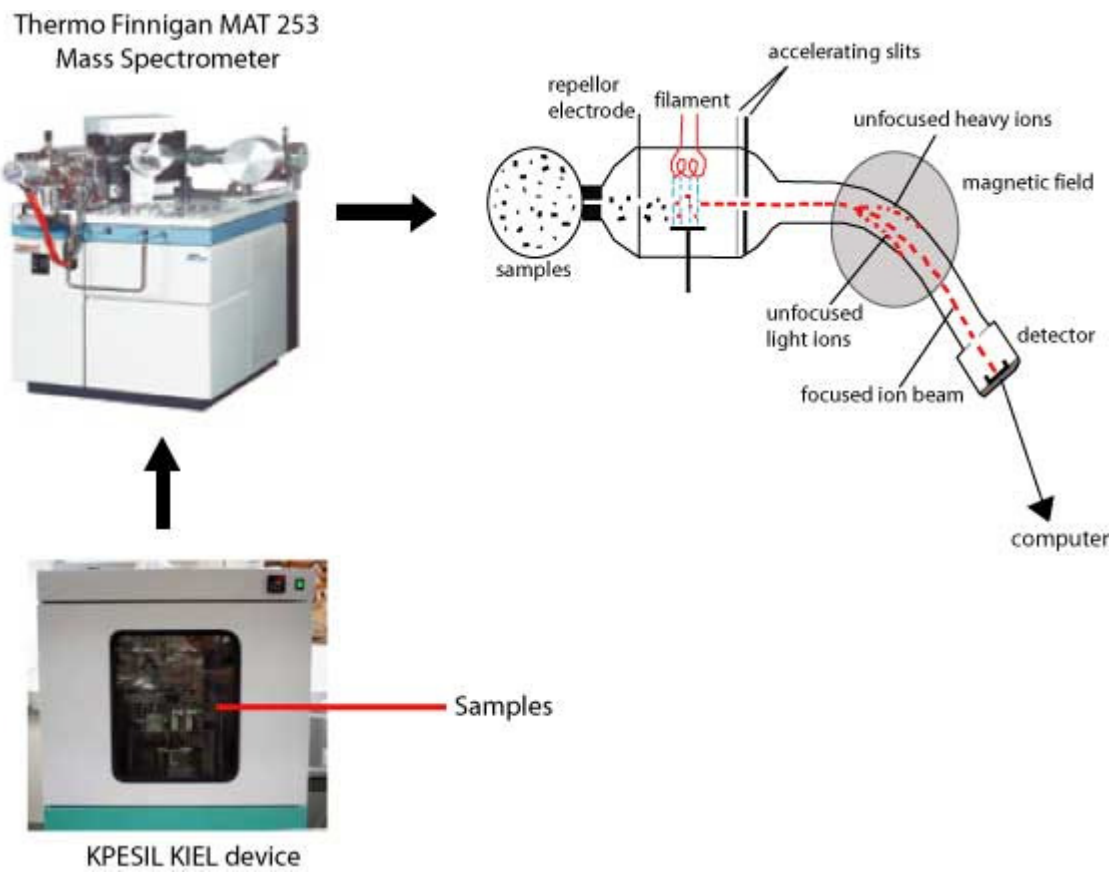


Figure 5: Isotopic method diagram. This diagram shows the process of isotopic analysis.

CHAPTER III

PREVIOUS STRATIGRAPHIC INVESTIGATIONS

A. General Stratigraphy of Bighorn Basin

The Bighorn Basin contains rocks ranging in age from Early Precambrian to Recent time including Cambrian sands, shales, and limestones, to Miocene and younger pyroclastic rocks (Figure 6). The total thickness of sedimentary rocks in the Bighorn Basin averages over 33,000 feet or 10,058 meters (Halverson, 1964). The Paleozoic and Mesozoic shelf sediments in the basin were deposited non-conformably above Precambrian granites, schists, and gneisses (Samuelson, 1974). Above this erosional nonconformity is a full section of 760 to 1000 meters of Paleozoic and 1950 to 3600 meters of Mesozoic sediments, which are in turn covered locally by perhaps as much as 4500 meters of Tertiary basin-filled sediments (Samuelson, 1974).

The sediments of Lower Precambrian, as old as 3.2 BY, have a total thickness of 3000 meters (Samuelson, 1974). The Cambrian System is represented by three formations in ascending order: the basal Flathead Sandstone, the Gros Ventre Formation, and the Gallatin Formation (Halverson, 1964). The Cambrian Flathead Formation (up to 60 meters thick) is composed of basal conglomerate and arkosic sands that overlie a weathered granite surface and grade into finer sand at the top (Halverson, 1964 and Samuelson, 1974). The Flathead Formation is overlain by Gros Ventre (150-180 m.) and Gallatin Formations (140-160 m.) (Samuelson, 1974). The Gros Ventre Formation consists mainly of glauconitic and sandy limestone with interbeds of dark grayish green shale and some limy sandstone (Mills, 1956). The Gallatin Formation is composed of glauconitic limestones and pebbly limestones with shale and some sandstone interbeds (Mills, 1956; Halverson, 1964).

The overlying Ordovician is represented by the massive Bighorn Dolomite (Halverson, 1964). This dolomite forms massive cliffs which are exposed on all sides of the basin (Samuelson, 1974). During the Silurian, Wyoming was entirely emerged so no Silurian rocks have been recognized (Mills, 1956; Halverson, 1964). The result is that the Bighorn Dolomite is directly overlain by the massive cliffs of the Devonian Jefferson Limestone and Three Fork Formations (Samuelson, 1974).

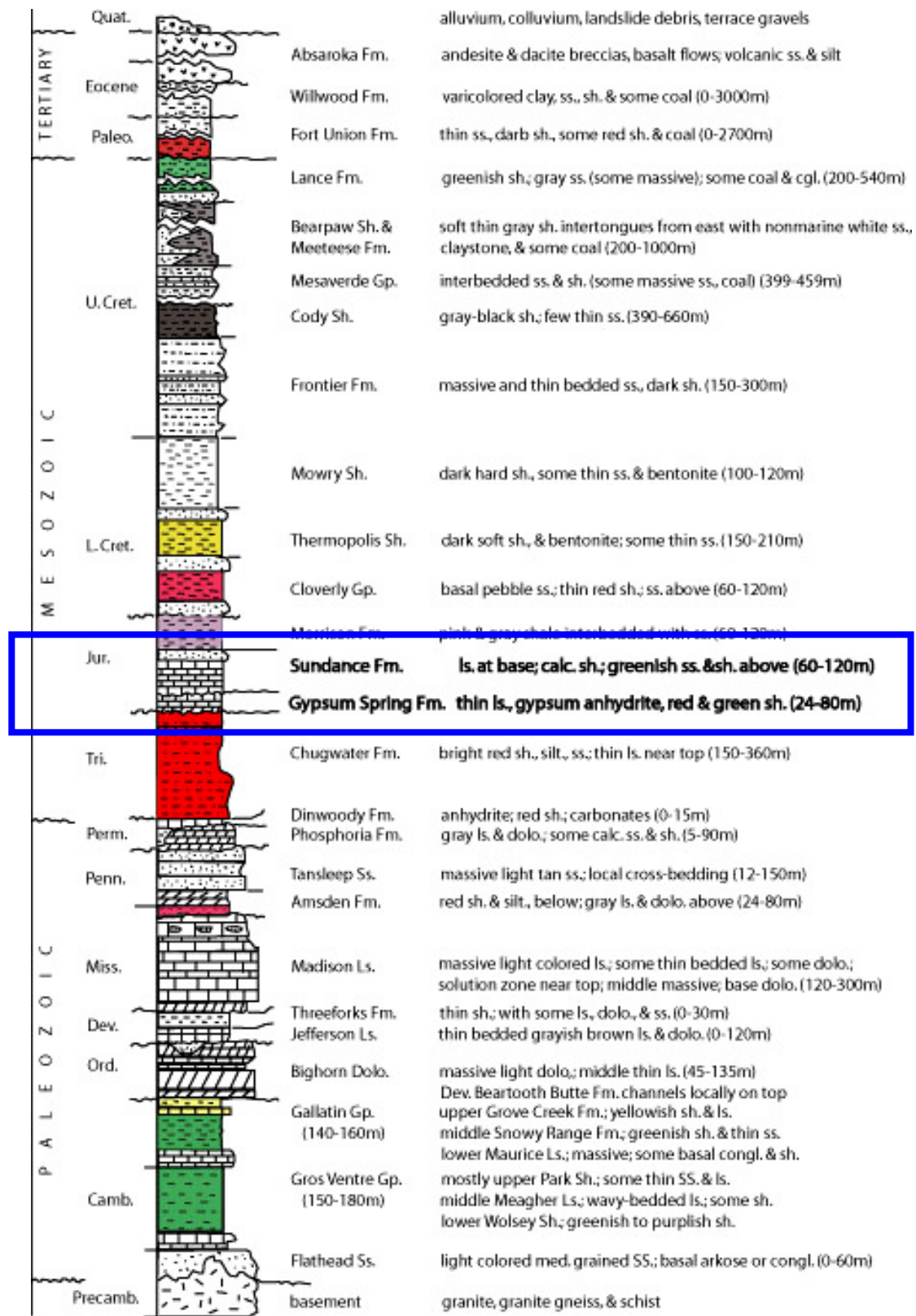


Figure 6: General stratigraphy of sedimentary deposits in Bighorn Basin. The emphasized box indicates rock units of interest which associated with Gypsum Spring and Sundance Formation. (Modified from Samuelson, 1974)

Over 120 meters of rocks assigned to Devonian age occur in the northern part of the Bighorn Basin (Halverson, 1964). The Devonian Jefferson Limestone and Three Fork Formations are relatively thin-bedded slope-forming limestones, dolomites, shales, and sands (Samuelson, 1974).

The major Paleozoic rock in the area is the Mississippian Madison Limestone (Samuelson, 1974). The Madison reaches a maximum thickness of 270 meters in the northern part of the basin (Mills, 1956; Halverson, 1964). The Madison Group consists of gray to brown fine crystalline limestone and fine sucrose dolomite (Mills, 1956). The Madison Limestone is an important oil reservoir in the subsurface Bighorn Basin. The lithology changes from the carbonates of Madison Group into the clastics of the overlying Amsden shaly unit.

The Amsden and Tensleep Formations comprise rocks of Pennsylvanian age. The Amsden Formation lies disconformably upon the karst topography on the Madison carbonates (Mills, 1956). The Amsden Formation can be divided into two units, an upper carbonate sequence and a lower shale and sand unit (Mills, 1956). The total thickness of the Amsden Formation ranges about 24 to 80 meters (Samuelson, 1974). Overlying the Amsden Formation is the Upper Pennsylvanian Tensleep (Quadrant) Sandstone, massive cliffs which reach 150 meters in thickness. The Tensleep Formation is composed of well-sorted fine to medium grain cross-bedded sandstone (Halverson, 1974).

Permian rocks of this area are represented by the Phosphoria Formation which includes a series of limestone, dolomite, chert, phosphate rocks, shales, and sandstone (Mills, 1956; Halverson, 1964). The Phosphoria Formation reaches a thickness of about 15 meters in the northern basin area (Halverson, 1964).

During the Mesozoic, the Bighorn Basin was influenced by numerous cycles of emergence and subsidence from relatively deep marine to shallow marine, tidal flat and continental environments (Samuelson, 1974). The Triassic contains the Dinwoody and Chugwater Formations (Halverson, 1964). The Dinwoody Formation is 15 to 30 meters thick (Halverson, 1964). The upper part of the unit consists of anhydrite with varying amount of red shale and very fine crystalline dolomite (Mills, 1956). Locally the anhydrite grades to anhydritic red shale and is underlain by a series of more red shales (Mills, 1956). The Triassic stratigraphy is dominated by the bright red Chugwater Formation, which was deposited during the Late Triassic emergence and overlies the Dinwoody Formation (Samuelson, 1974). The Chugwater

Formation is a series of red to maroon sands, shales and minor limestones and can be divided into three members (Halverson, 1964): 1) the lowermost Red Peak Member is 127-230 meters of unfossiliferous, predominantly red and maroon shale with locally abundant green mottling and salmon to red siltstone (Mills, 1956 and Halverson, 1964). 2) The Alcova Limestone Member is the middle unit. The total thickness does not exceed 5 meters. This limestone is locally absent by truncation, due to or by a local facies change to sandstone (Mills, 1956). 3) The Crow Mountain Member is massive gray cliff-forming sandstone (Love, 1939). Grain size is fine to medium with scattered medium to coarse sand grains (Mills, 1956). Thickness ranges from 13-23 meters (Mills, 1956). The Crow Mountain, Alcova and portions of the Red Peak are lost due to erosional truncation. This truncation causes a loss of Triassic section from over 360 meters on the south to less than 150 meters at the north end of the basin.

The Jurassic System is made up of many different depositional environments and rock types. The Gypsum Spring Formation can generally be divided into two units throughout the Bighorn Basin (Mills, 1956). These units consist of an upper shale and carbonate sequence, and a lower anhydrite interval. The carbonates of the upper unit consist of gray, black, and brown limestone, and white or cream dolomite (Mills, 1956). Shale interbeds are red, maroon, and green in color. Green shales are most prominent near the top of the Gypsum Spring Formation (Mills, 1956). The lower unit consists predominantly of anhydrite, usually white in color and micro-crystalline to fine crystalline (Mills, 1956). The average thickness of Gypsum Spring Formation is around 65 meters (Mills, 1956; Halverson, 1964). The Gypsum Spring Formation consists of evaporitic sediments that formed during the Middle Jurassic, and it is overlain by limestone and greenish gray shales of Sundance Formation (Samuelson, 1974). The Sundance Formation in the Bighorn Basin can be divided into two major units, the "Upper Sundance" and "Lower Sundance" (Mills, 1956). The Lower Sundance rocks consist of interbedded sandstone, limestone and shale. Sandstone most commonly occurs near the top (Mills, 1956). The Upper Sundance Formation consists predominantly of sandstone with interbedded shales and some limestone (Mills, 1956). Many dinosaur-fossil localities are found in the basin, including the Upper Jurassic Morrison Formation. The Morrison consists of interbedded sandstone, claystone, and scattered limestone beds (Mills, 1956; Halverson, 1964). Siltstones, conglomeratic sandstone, and conglomerates are irregularly present throughout the section (Mills, 1956; Halverson, 1964). Thickness averages around 60 meters.

The Cretaceous rocks in the Bighorn Basin are mostly shallow marine and continental shales and sands such as Thermopolis Shale, Mowry Shale, Frontier Formation, and Cody Shale (Samuelson, 1974). Lower Cretaceous rocks in the Bighorn Basin include the Cloverly Group, Thermopolis Shale, Muddy Sandstone, and Mowry Shale (Mills, 1956; Halverson, 1964). The Cloverly Group can be divided into three units: 1) a basal Pryor and Lakota conglomerates consist of conglomerates, sandstones, conglomeratic sandstones, siltstone, and thin interbeds of inclusions of varicolored shale (Halverson, 1964). Thicknesses vary from 3 meters to 33 meters in the basin. 2) A middle shale unit of varicolored shale and claystone with minor sandstones and siltstones. 3) The Greybull Sandstone, a lenticular sandstone (Halverson, 1964). The Thermopolis Shale, bounded by the Greybull Sandstone below and the Muddy Sandstone above, can be divided into three units (Mills, 1956). These include upper shale, middle unit silt, and a lower silt and sand. The middle silt is correlative with the "Dakota Silt" in Montana, and the lower unit is called the "Rusty Beds" (Mills, 1956). The Mowry Shale consists of dark gray to black silicious shale with abundant beds of white bentonite and fish scales (Mills, 1956 and Halverson, 1964). Thickness average is about 111 meters throughout the basin (Halverson, 1964).

The Upper Cretaceous rocks are represented by the Frontier Formation, Cody Shale, Mesaverde Group, Meeteetse-Lewis-Bearpaw interval, and the Lance Formation (Halverson, 1964). The Frontier sequence consists of conglomerates, sandstone, shale and bentonite beds (Halverson, 1964) and is apparently constant along the west side of the Bighorn Basin. Frontier Sandstone is an important source for oil and gas (Mills, 1956) with some coal deposits as well (Samuelson, 1974). The Cody Shale is composed of a thick series of gray to medium gray shale with minor interbeds of silty shale, siltstones, and fine sandstones (Mills, 1956). The formation thickens from 420 meters in the northwest part of the basin to over 630 meters on the southeast side (Halverson, 1964). The Mesaverde sequence is a cliff-former consisting of a sand, shale, and thin coal bed sequences (Halverson, 1964). The Meeteetse Formation overlies the Mesaverde in the western part of the basin. The thickness of the interval ranges from about 210 meters to 450 meters (Halverson, 1964). The Lance Formation of latest Upper Cretaceous age is generally composed of terrestrial sands, shales, and coals (Halverson, 1964).

Early Cenozoic sediments are Paleocene to Eocene alluvial deposits which are overlain by Absaroka volcanics. The Absaroka volcanics accumulated from Middle Eocene to Late Eocene time (Samuelson, 1974). The Fort Union Formation of Paleocene is composed of sand and shale sequences containing some coal zones (Halverson, 1964). The thickness ranges from about 390 meters to 2400 meters in the center of the basin (Halverson, 1964). The Willwood Formation of Eocene consists of a series of sandstones, claystones and shales (Halverson, 1964). In the central region of the Bighorn Basin there are several elevated terraces, or benches, of Pleistocene through Recent ages (Halverson, 1964). The volcanic derived rocks on the west side of the basin (Absaroka Plateau) range in age from Eocene to Miocene and younger, and consist of volcanic derived sediments, igneous flows and intrusive dikes, sills and plugs (Halverson, 1964). There are also the deposits of alluvial, landslide debris and terrace gravels of Quaternary sediments on top of these Tertiary sediments (Samuelson, 1974).

B. Middle Jurassic Stratigraphy of Northwestern Wyoming

The Jurassic System in northwestern Wyoming is made up of many different depositional environments and rock types. Rock units of interest to this study are associated with the Gypsum Spring, and Sundance Formations. The Middle Jurassic rocks of the Bighorn Basin record several major tectonic events. The effects of these events on deposition are expressed by large scale unconformities and the varied compositions of the rocks left behind. These deposits reflect marine and brackish waters that invaded the Western Interior region from the early Bajocian to early Callovian (Schmude, 2000).

The oldest Jurassic rocks in the study area are the Gypsum Spring Formation which overlies the Triassic Chugwater Group. The Gypsum Spring Formation is bound at the base by the J-1 unconformity and at the top by the J-2 unconformity (Schmude, 2000). The J-1 unconformity is the most significant unconformity in the Mesozoic sequence of the Bighorn Basin. It separates Middle Jurassic rocks from the underlying Triassic Chugwater Group (Schmude, 2000). Because the J-1 unconformity underlies the Gypsum Spring, the unconformity only occurs where the Gypsum Spring Formation is present (Johnson, 1991). Stratigraphic relationship of sedimentary deposits of the Middle Jurassic in the Bighorn Basin is shown in Figure 7.

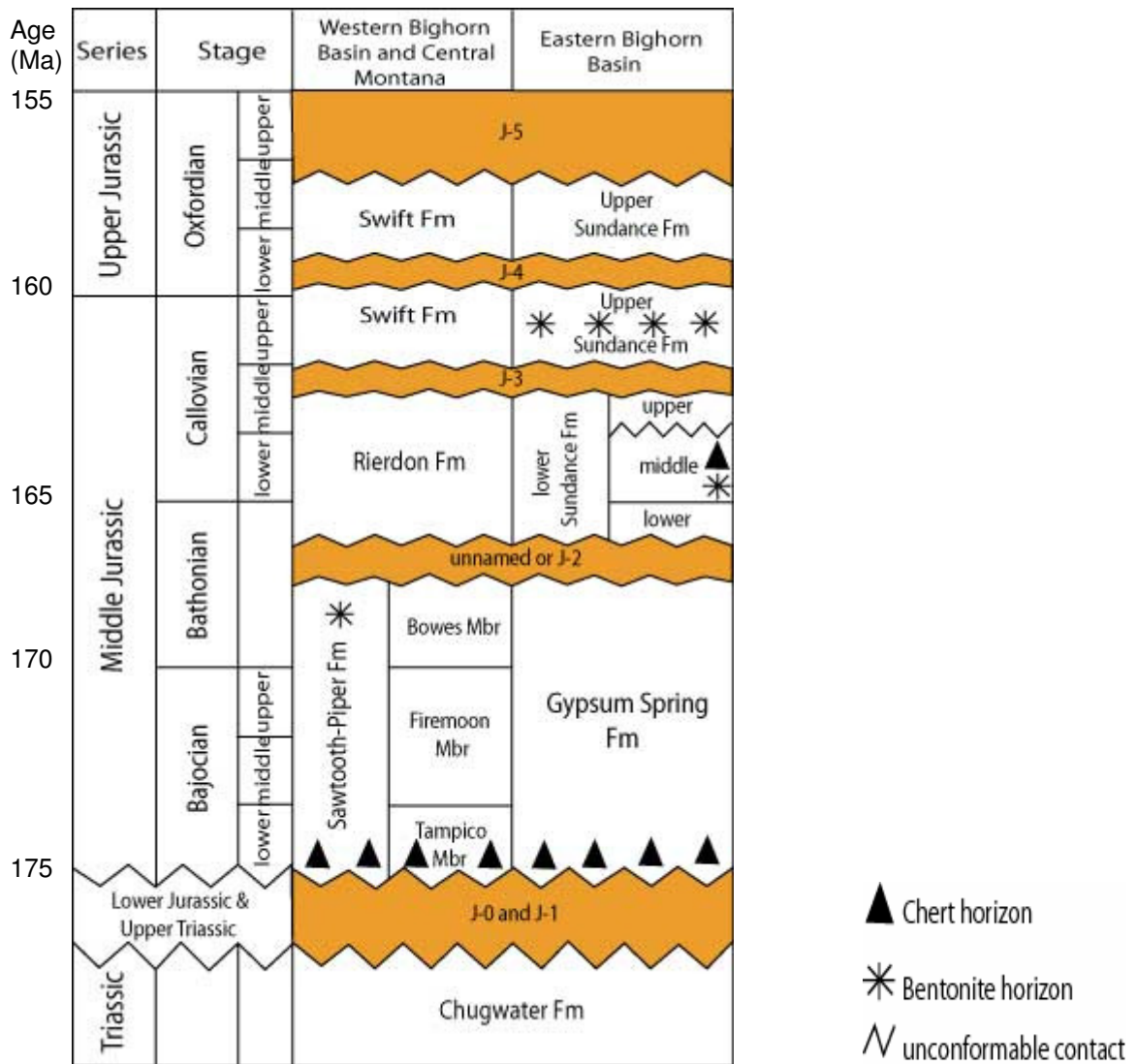


Figure 7: Stratigraphic relationship of Middle Jurassic rocks in the Bighorn Basin
 (after Parcell and Williams, 2002)

1) Gypsum Spring Formation

The Gypsum Spring Formation was deposited during the Early Bajocian (Imlay, 1980; Johnson, 1991). Love (1939) first described the Gypsum Spring Formation as a 76 meter-thick section of gypsum, red shale, and carbonate rocks. The Gypsum Spring Formation along the east side of the Bighorn Basin is about 62 meters thick at the Sykes Mountain and thins southeast to Nowood where it pinches out southward along the flanks of the Bighorn Mountains (Halverson, 1964). The Middle Jurassic section in Park County, Wyoming (west side of Bighorn Basin), ranges in thickness from 52 to 97 meters (Halverson, 1964). This formation is generally comprised of red shales, carbonates, and anhydrites/gypsum. The Gypsum Spring Formation of Wyoming includes a lower section of massive gypsum and red shale and a middle unit of interbedded of gray, black, and brown limestone, white or cream dolomite, green and red shale, with some gypsum, and an upper unit of red shale that locally contains minor amounts of gypsum (Peterson, 1957; Imlay, 1956). Gypsums beds are common near the base and gypsum nodules occur throughout the section (Imlay, 1956).

The lower member of the Gypsum Spring sequence consists of massive white gypsum 15 to 24 meters thick, overlain by soft dark brownish red claystone and siltstone 4 to 10 meters thick (the gypsum is absent at some localities) (Imlay, 1956). Imlay (1956) also described the middle member of Gypsum Spring in Park County as a section that consists mostly of interbedded gray to yellowish gray limestone and gray to greenish gray fissile claystone and ranges in thickness from 23 to 30 meters. The limestones of this middle member vary from thin to thick bedded, from a few centimeters to 5 meters in thickness, and may be dense, granular, oolitic, coquinoid, or even sandy in rare instances (Imlay, 1956). Coquinoid and oolitic limestones occur throughout the member; however coquinoid beds are most common in the lower part (Imlay, 1956). In Park County the upper member of the Gypsum Spring ranges from 17 to 27 meters in thickness and consists mostly of soft brownish red claystone with some greenish gray layers at most localities.

Upper Contact of Gypsum Spring

After the deposition of the Gypsum Spring Formation, uplift, regression and significant erosion formed the J-2 unconformity (Schmude, 2000). The upper limit of the Gypsum Spring is not a consistent or standardized boundary and varies between localities (Mills, 1956). In eastern Wyoming the J-2 unconformity is an angular unconformity which overlain by the lower part of Sundance Formation (Johnson, 1991). The contact is placed anywhere between the basal Sundance oolitic limestone of higher energy marine, and the top of the basal anhydrite unit, including red and green shales which is the restricted marine (Meyer, 1984; Halverson, 1964). This contact represents the change from the regressive phase to the transgressive phase of the third major marine transgression into the Western Interior (Meyer, 1984).

In Park County, Wyoming, Imlay (1956) placed the contact at the top of redbeds (upper member of Gypsum Spring), which are overlain sharply at all localities by fossiliferous soft gray fissile claystone or by fossiliferous gray oolitic to nodular limestone at the base of the Lower Sundance formation. This abrupt change of lithology indicates environmental change but Imlay (1956) did not believe that it is proof of an unconformity at the contact. Contrary to Imlay, Mills (1956) placed the contact anywhere between basal Sundance oolitic limestone and the top of the basal anhydrite unit.

2) Sundance Formation

The Sundance Formation of the Bighorn Basin can be divided into two major units, the Upper Sundance and Lower Sundance (Halverson, 1964). The Lower Sundance beds lay disconformably on top of Middle Jurassic Gypsum Spring rocks in the study area and are considered Callovian in age, and the Upper Sundance rocks are considered Oxfordian in age (Halverson, 1964). This study emphasizes only the Lower Sundance Formation which is related to the formation of the microbial buildups.

The Lower Sundance rocks consist of interbedded minor or non-glaucconitic sandstone, siltstone, oolitic limestone, and gray to green-gray limy shale with some red or maroon varicolored. The most common colors of the sands are light gray, gray, and white and most limestones are white, gray, tan, and brown (Peterson, 1957 and Halverson, 1964). Texture is generally micro-crystalline to lithographic and quite often fragmental (Halverson, 1964). The lithology of the Lower Sundance Formation that is exposed in Park County is identical with the Lower Sundance Formation in the Yellowstone National Park area

(Imlay, 1956). The formation in Park County includes a basal unit of alternating oolitic limestone and calcareous claystone followed by a much thicker layer of soft fissile gray calcareous claystone that contains an abundance of *Gryphaea nebrascensis* (Imlay, 1956). The Upper Sundance Formation is composed of Redwater Shale and Windy Hill Sandstone Members. In Park County, the Upper Sundance Formation consists mostly of highly glauconitic calcareous sandstone and contains more belemnites in the lower part (Imlay, 1956).

CHAPTER IV

THE FIELD/OUTCROP LITHOLOGY

The examined marine Jurassic rocks are located in the Bighorn Basin of north western portion of Wyoming. The microbial buildups of interest are located along the east side of Cedar Mountain at 14-T52N-R102W in Park County, south of Cody, Wyoming (Figure 1, Figure 2 and also Figure 8). The town of Cody lies at the southeast base of Rattlesnake Mountain along the Shoshone River, within the western shoulder of the Bighorn Basin (Spearing, and Lageson, 1988). Rattlesnake and Cedar Mountains extend in a southwest direction, about 15 miles beyond Cody, resulting from the large anticline uplift (Ziegler, 1917). The studied microbial outcrop lies along a contact between Gypsum Spring and Lower Sundance Formation (Figure 9). The studied microbial section is semi-circular in shape, 2.27 meters in height, 2.9 meters width and 30 centimeters in thickness (Figure 10 and 11). These microbial mounds are not a complete section. The top of the unit has been removed by erosion, although neighboring mounds are complete to the top of the section. The microbial buildups are composed of several thrombolite heads. Each head has a circular shape with the average minimum diameter ranging from 20 centimeters up to 60 centimeters; and the maximum diameter ranging from 30 centimeters up to 70 centimeters.

The classification of carbonate lithologies and texture of rocks is based on Dunham's (1962) classification. The total thickness of the measured section is about 49.50 meters and the microbial build ups that formed on top of this unit have a thickness of about 30 centimeters with semi-circular in shape and around 290x227 cm in diameter. The measured microbial buildup is composed of about 30 heads. The individual heads have a variety in shape such as oval, circular, and semi-circular with diverse sizes (Table 1).

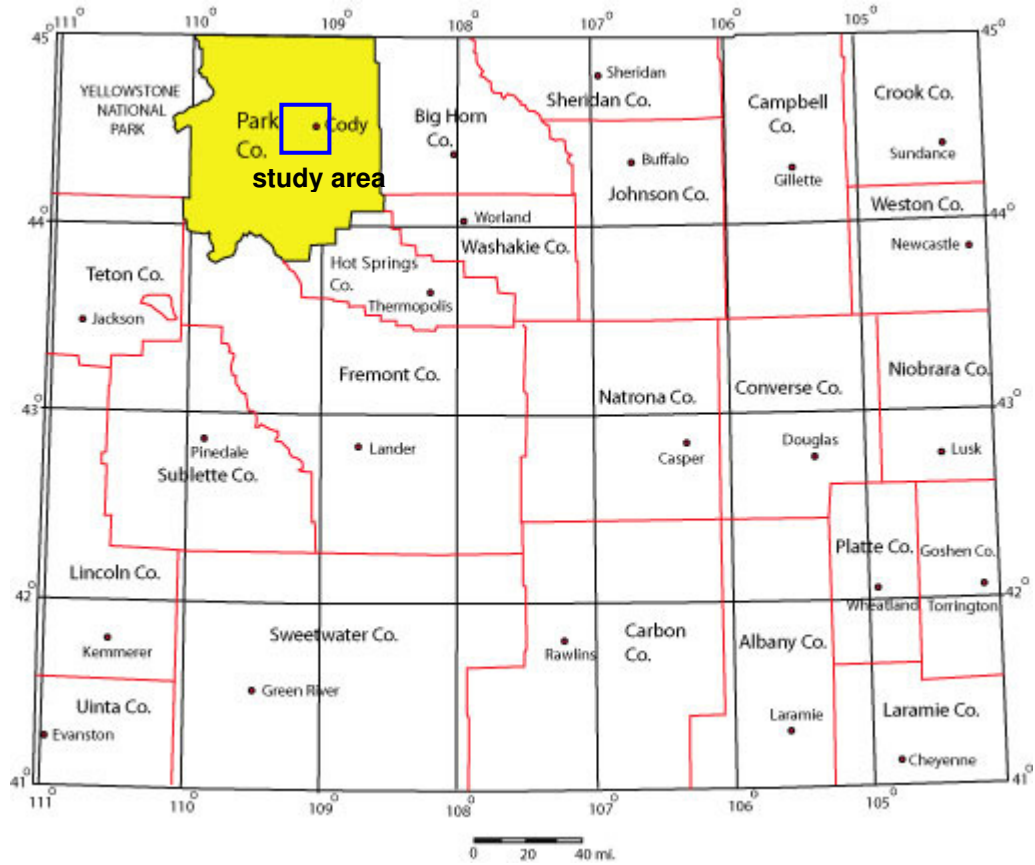


Figure 8: Location of study area in Park County, Wyoming

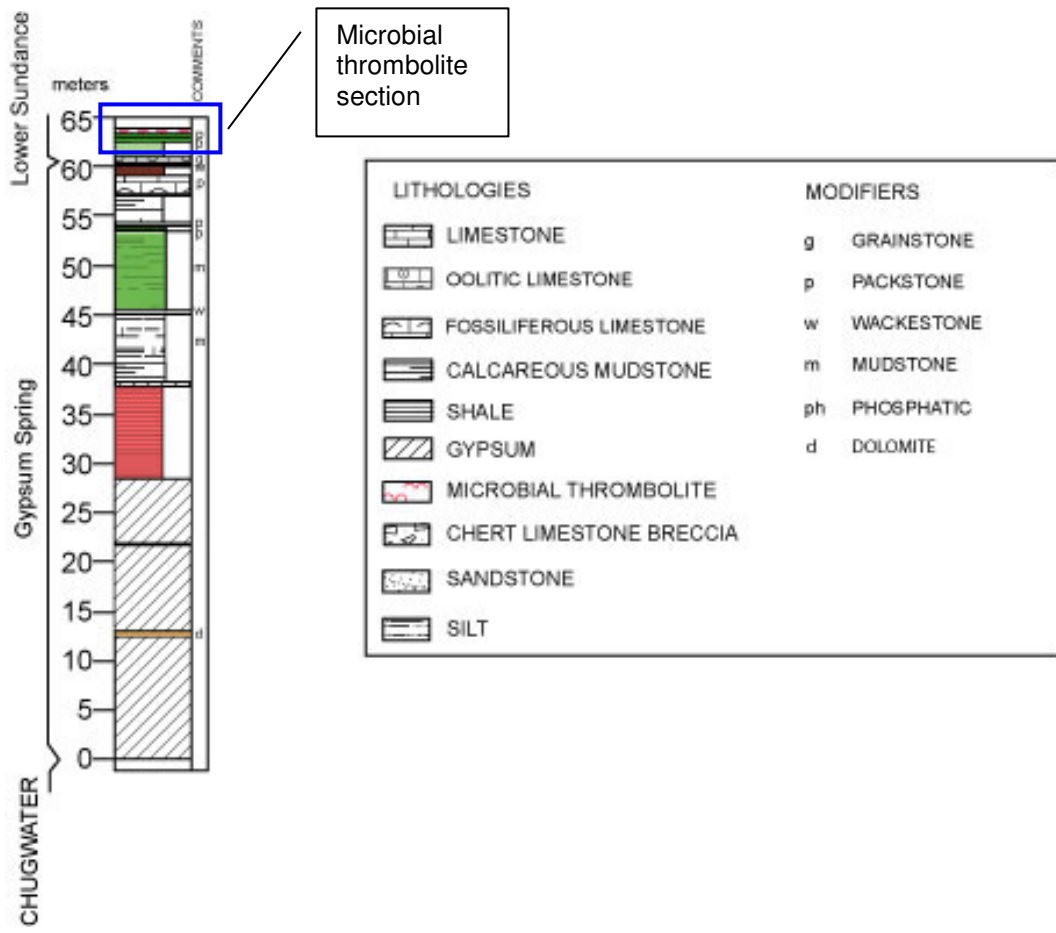


Figure 9: The studied microbial outcrop lies along a horizon at the contact between the Gypsum Spring and Lower Sundance Formation



Figure 10: Microbial buildup outcrop containing 30 individual heads of thrombolites.

Note: Outcrop is tilted from original position. Photo is a top view of unit.

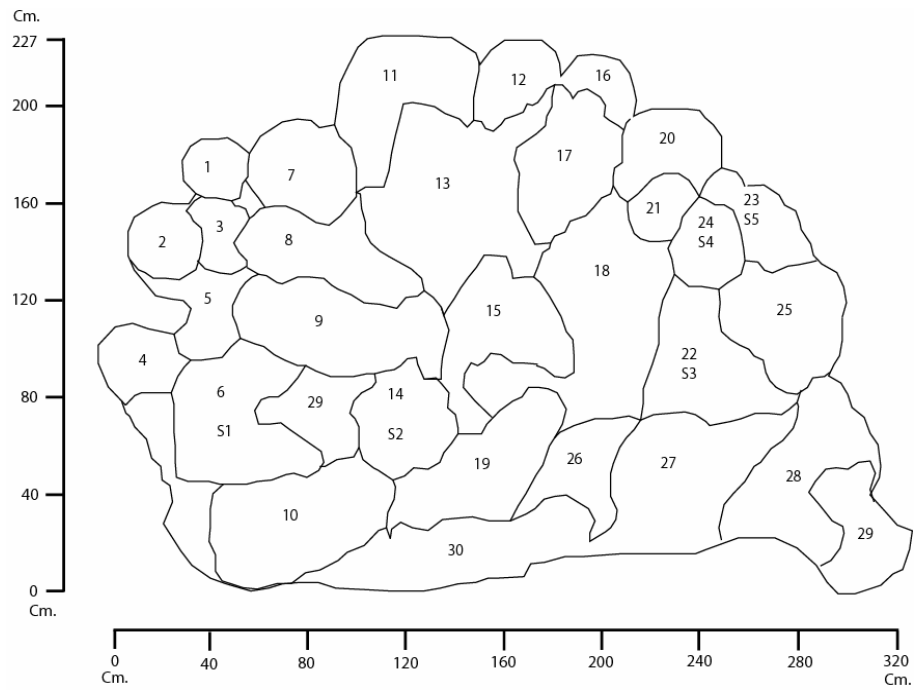


Figure 11: Top view of microbial outcrop including scale in cm

Table 1: This table indicates sizes of microbial buildup heads from the outcrop

Microbial Head No#	Maximum Diameter (cm)	Minimum Diameter (cm)	Microbial Head No#	Maximum Diameter (cm)	Minimum Diameter (cm)
1	22	18	16	30	13
2	31	29	17	55	35
3	17	27	18	60	47
4	32	26	19	28	25
5	25	20	20	31	22
6	47	32	21	26	25
7	35	23	22	68	40
8	45	30	23	24	17
9	65	30	24	34	27
10	73	35	25	68	60
11	65	26	26	70	49
12	35	30	27	68	36
13	72	58	28	32	20
14	32	32	29	35	25
15	44	20	30	34	32

A. Stratigraphy of Gypsum Spring Formation

The lithology of the Gypsum Spring Formation includes gypsum, dolomite interbedded with shale, and mudstone at the base. At the top of the formation wackestones dominate and are interbedded with packstone and shales. The studied section, located east of Cedar Mountain, is shown in figure 12. The lithology of the Gypsum Spring is shown in the stratigraphic section of figure 13. The total thickness of the Gypsum Spring Formation is about 46 meters. The detailed description of lithologies from the Gypsum Spring Formation, including their textures and color characteristics under binoculars, are shown in Appendix A and Appendix B.

1) Gypsum facies

Starting from the base of the studied Middle Jurassic section, gypsum is the most dominant lithology in the Gypsum Spring Formation. This gypsum (Figure 13) varies in thickness from a couple centimeters to several meters. The thickness of these gypsums indicates the depth of the water when they were deposited. The basal 60 centimeters thickness of massive white gypsum interbedded with light gray colored dolomite (N7). They are a crystalline texture. These fine grained, or microcrystalline textures, represent a relatively rapid precipitation of gypsum. The top of the unit is covered. The thinner beds of gypsum are most commonly interbedded with dolomite and color bands such as reddish brown (5YR 4/4) and yellowish red (5YR 5/6). Some gypsum units are interbedded with shaly siltstones. The upper sections of gypsum are gradually scattered within other lithologies such as shale. Gypsum at the lower unit is massive and at the upper unit is thickly bedded with nodule.

2) Dolomite facies

Dolomites are another of the common lithologies found at the base of the Gypsum Spring Formation. Light gray color dolomite (N7) often interbeds with gypsum. Its thickness ranges from a couple centimeters to about 60 centimeters. These dolomites are fine to crystalline grained size. Dolomite also interbeds with shaly siltstone. Some of the dolomite is only 1 cm thick or forms as a lens at the top of the gypsum unit. Dolomite that has interbedded with gypsum has reddish brown color bands. Dolomite tends to form at the surface on supratidal flats a few centimeters above normal high tide (Shinn, 1983).

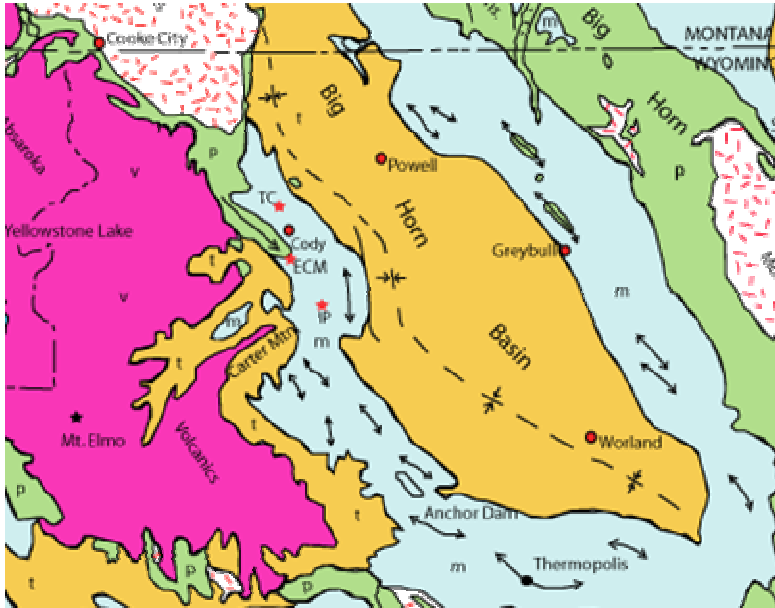


Figure 12: This map indicates location of sections near Cody from Middle Jurassic in the Bighorn Basin; Trail Creek section (TC), East of Cedar Mountain section (ECM) and Indian Pass Quadrangle section (IP).

(Note: The index of this figure is the same with figure 1)

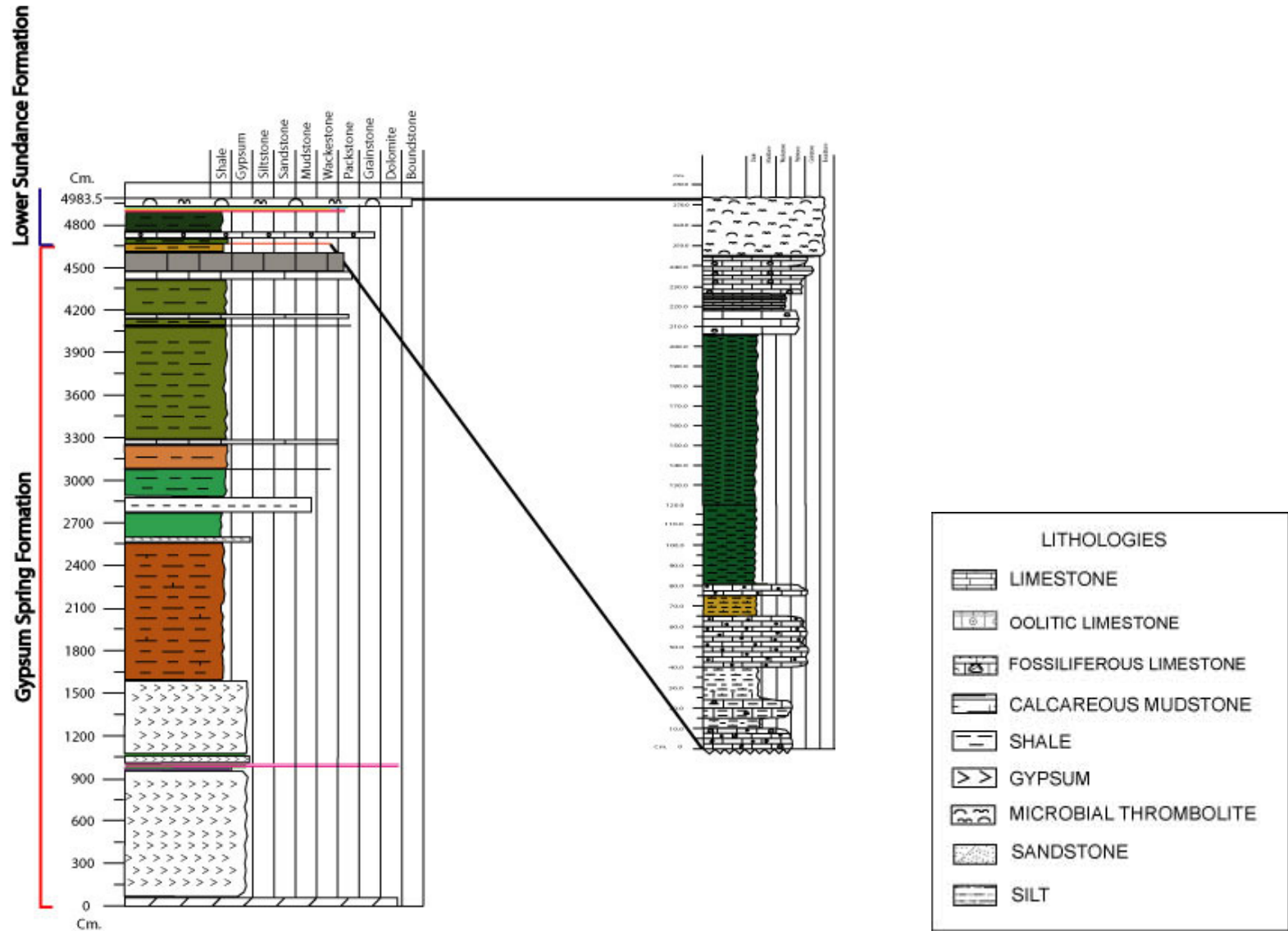


Figure 13: Stratigraphy of Middle Jurassic (Gypsum Spring and Sundance Formation) of study area (east of Cedar Mountain)

3) Reddish to brown shale facies

At the middle of the Gypsum Spring Formation, there are several beds of shales. On top of those lower gypsum units, there is 9.7 meters of covered blockly red shale (5YR 3/4) along with some gypsum. These shales are weak calcareous and have hard-to-see bedding. Reddish shale lithology is also found at the upper unit of Gypsum Spring Formation. They interbed with carbonate lithology. The top unit of the Gypsum Spring Formation is grayish brown shale (10YR 4/2) which is mostly covered. These dark grayish brown shales (Imlay, 1956), referred to as redbeds, at the top of the Gypsum Spring in Park County represent the contact between Gypsum Spring and Lower Sundance Formation. They are overlain sharply by fossiliferous gray oolitic limestone at the base of the Lower Sundance Formation. According to Imlay (1956), such an abrupt lithologic change may be evidence of an environmental change.

4) Gray-green shale facies

Gray-green shale/olive-gray shale (5Y 5/2, 5Y 7/2) are mostly found at the upper section of the Gypsum Spring Formation; however, there are several beds of gray-green shale at the middle unit of Gypsum Spring. Most gray-green shales are covered and interbedded with carbonate lithologies such as lime mudstones, wackestones, and grainstones. The average thickness of gray-green shale is between 1.9 to 2.5 meters. Few fossils are present in these shales. Near the top these shales include limestone and gypsum stringers.

5) Lime mudstone facies

Not many lime mudstone facies are found at the middle unit of Gypsum Spring Formation. There is one meter thick of gray-tan color mudstone, which contains pelecypod shell fragments.

6) Wackestone and packstone facies

Most of wackestone and packstone are concentrated in the uppermost unit of Gypsum Spring Formation. Their thickness is between 2 centimeters up to 1.4 meters, and gray color is common. There are a couple of thin beds of packstone which contain an abundance of crinoids and pelecypod shell fragments. At the very top of Gypsum Spring, there is packstone. This unit is loosely consolidated material and is composed of small crinoids and pelecypod shell fragments. The top surface is highly

bioturbated and contains several large shrimp burrows. This surface unit contains many types of organisms such as gastropods, pelecypods, and ostracods.

B. Lithology of Lower Sundance Formation

The stratigraphy of the Lower Sundance Formation (Figure 13) can be divided into several lithofacies. The Lower Sundance rocks consist of interbedded sandstone, limestone, and shale. Although, in this studied outcrop, there are only dominant shale and limestone beds.

1) Olive-brown shale facies

At the base of the Lower Sundance Formation there are 30 centimeters of light olive brown shale (5Y 5/6). This calcareous shale is loosely consolidated and interbedded with a thin bed of packstone (ECM MP2) (Figure 14).

2) Gray-green shale facies

At the middle unit of the Lower Sundance Formation there are 1.25 meters of greenish shale (10Y 6/2). This shale is loosely consolidated, partially covered, with no fossils found.

3) Lime Mudstone facies

There are 8.5 centimeters of laminated to very thin bedded mudstone. This mudstone (ECM MP6) has medium gray to light brown color and is also composed of whitish powder of calcite (Figure 15). Animal tracks and trails are also found in this mudstone. Lime mudstone is also found at the base of the microbial thrombolite section. This medium gray mudstone (ECM MP9) is a substrate of microbial thrombolite (Figure 15).

4) Wackestone and packstone facies

There are several beds of packstone in the Lower Sundance Formation. At the base of this Formation there is a thin bed (10 cm) of fossiliferous packstone (sample ECM MP1) (Figure 16), whitish gray weathered color and light gray to medium gray fresh color. This packstone is a ledge formed with high bumpy and rough surfaces. It contains pelecypods (*Homonya gallatinesis*), gastropods, oolites, and also some small circular depressions. The upper unit is 30 cm thick of calcareous shale interbedded with a thin bed of dense wackestone to packstone (sample ECM MP2). This packstone contains pelecypods, some oolites, and other microorganisms. There is one particular bed of packstone that differs from the



Sample: ECM MP2

30 cm. Interbeds of loosely consolidated 5y 5/6 light olive brown (wet) calcareous shale and thin bedded of dense wacke-packstone contained pelecypods, weathered orange brown-medium gray, freshed light gray slightly orange brown

Figure 14: Facies 1: olive-brown shale lithology (ECM MP2) and Facies 2: wackestone and packstone (ECM MP2) from Lower Sundance Formation at east of Cedar Mountain



Sample: ECM MP6
8.5 cm. Laminated-very thin beds of mudstone, weathered light gray, freshed dark gray to light brown, contained whitish powder of calcite and track & trail



Sample: ECM MP9
This sample is a substrate directly underneath microbial mounds. It is a medium gray mudstone.

Figure 15: Facies 3: lime mudstone lithology (ECM MP6, ECM MP9) from Lower Sundance Formation at east of Cedar Mountain



Sample: ECM MP1

10 cm. Thin beds of fossiliferous dense wackestone-packstone, bumpy surface, ledge former contained pelecypods (*Homomya gallatinesis*) and gastropods, weathered whitish gray, freshed light-medium gray



Sample: ECM MP2

30 cm. Interbeds of loosely consolidated 5y 5/6 light olive brown (wet) calcareous shale and thin bedded of dense wacke-packstone contained pelecypods, weathered orange brown-medium gray, freshed light gray-slightly orange brown



Sample : ECM MP 5

12 cm. Medium beds of fossiliferous packstone, weathered dark gray to orange brown, freshed dark gray with some orange to dark brown, contained small pelecypods, strike 52 S, dip 58 S



Sample: ECM MP7

9 cm. of thin bedded packstone slightly ledge former and partly cover up /overlap on top of the microbial mounds, medium gray to orange brown in weathered color, dark brown with some yellowish freshed color, contain slightly of calcite powder, composed of shell fragments mostly pelecypods

Figure 16: Facies 4: wackestone and packstone lithology (ECM MP1, ECM MP2, ECM MP 5, and ECM MP 7)
from Lower Sundance Formation at east of Cedar Mountain

other. This packstone is sandy packstone (ECM MP5) with gray to orange brown color (Figure 16). This sandy packstone contains several small pelecypods. There are a couple beds of packstone that are overlain by microbial thrombolite. These packstone beds are thin bedded, 8 and 9 centimeters thick, and are found very close to the microbial thrombolite section. One bed of the packstone is partly covered up on top of the microbial mounds (ECM MP7) (Figure 10). They are also composed of many microfossils and shell fragments.

5) Grainstone facies

The oolitic grainstone is found at the lower unit of the Lower Sundance Formation (Figure 17). This bed is 41 centimeters thick and found interbedded with yellowish-brown shale. The lower part is 26 cm of medium bedded oolitic grainstone (ECM MP3), weathered light brown to light gray, fresh dark brown (rusty). The upper contact of oolitic grainstone is gradually changed to thin bed of yellowish brown shale (10YR 5/4) (wet). This shale is overlain by another bed of 5 centimeters of oolitic very dense packstone to grainstone.

6) Microbial thrombolite Facies (ECM S1 to S5)

The microbial buildups, or thrombolites mounds, are the top units of the Lower Sundance Formation. These microbial buildups form a thrombolitic or clotted fabric. The clotted fabrics are easily distinguishable in the field. The mounds are composed of several individual thrombolitic heads with a medium to light gray weathered color and a yellowish brown to dark brown fresh color (Figure 18). The microbial mounds contain microfossils and microorganisms, possibly bacteria, and also a dark color of organic matter. Most of the microbialite samples are high calcareous with microcrystalline texture. No fossils can be seen with the naked eye except for some samples which contain ostracods with a lot of burrows. Some samples contain a black color vein of mineral. Microscopically, they show three main types of microfabrics: dense, clotted, and peloidal micrites. The microscopic details will be explained later in the petrographic analysis section. There is an abundance of *Gryphaea* contained in shales which overlay this section. This gray green shale is not overlain directly on top of the microbial thrombolites section. There is an unconformity occurring after the microbial thrombolites deposition.



Sample: ECM MP3

26 cm. Medium beds of very dense oolitic packstone-grainstone, weathered light brown to light gray, freshed dark brown (rusty), strike S45E, dip 65S

Figure 17: Facies 5: grainstone lithology from Lower Sundance Formation at east of Cedar Mountain



Sample: S1 to S5

Microbial thrombolite samples with clotted surface and contain several heads, medium to light gray weathered color, yellowish brown to dark brown fresh color, composed of dark color of organic matter microfossils and probably bacteria.

Figure 18: Facies 6: microbial thrombolite lithology (ECM S1, S2, S3, S4, and S5)

C. Stratigraphic Analysis

1) Cross-section correlation

Comparison of stratigraphic cross-sections from three locations at Trail Creek (TC), east of Cedar Mountain (ECM) and Indian Pass Quadrangle (IP) (Figure 12 and 19) indicate variation of stratigraphy and lithology in each location. In general, the Gypsum Spring Formation of Trail Creek is the thickest section compared to the others whereas east of Cedar Mountain is the thinnest section. The gypsum at the base of this formation also varies in thickness. East of Cedar Mountain gypsum has greatest thickness which was likely caused by a high evaporation rate with high concentration of calcium sulfates in the water and also formed in high accommodation space. Evaporite deposition may be caused by many factors including high temperature, low humidity. The geographic distribution of modern evaporites tends to occur in low mid-latitudes under descending limb of the Hadley circulation (Parrish, 1998) which matches well with the paleogeographic location of Wyoming in the Jurassic Period. Gypsum gradually gives way to red shale which is easily seen by the mixing of some gypsum within the red shale. Probably increasing water influx introduced clastics and abundant terrestrial organic matter caused deposition of the red shale. The first unit of red shale deposited on top of the gypsum is thickest at east of Cedar Mountain outcrop compared to neighboring outcrops.

The middle unit of Gypsum Spring at all three locations is composed of shales interbedded with carbonate rocks which include mudstone, wackestone, and packstone with some fossils. The east of Cedar Mountain outcrop tends to be highly fossiliferous near the middle and top of the Gypsum Spring Formation. Furthermore, east of Cedar Mountain does not have thick red shale deposited at the top of the formation like the others. Instead, it has more carbonate deposited. The reddish shale of the studied section appears to pinch out from the other locations. The contact of the Gypsum Spring and Lower Sundance Formation is represented by oolitic grainstone deposition. This type of deposition indicates the stratigraphic sequence changing into a higher energy environment during the transgression of sea water.

At the beginning of the Lower Sundance Formation deposition, carbonate lithology is deposited at east of Cedar Mountain. This includes lime mudstone, highly fossiliferous wackestone and packstone. In the upper section of Lower Sundance Formation, there is an incomplete section of thrombolite. They

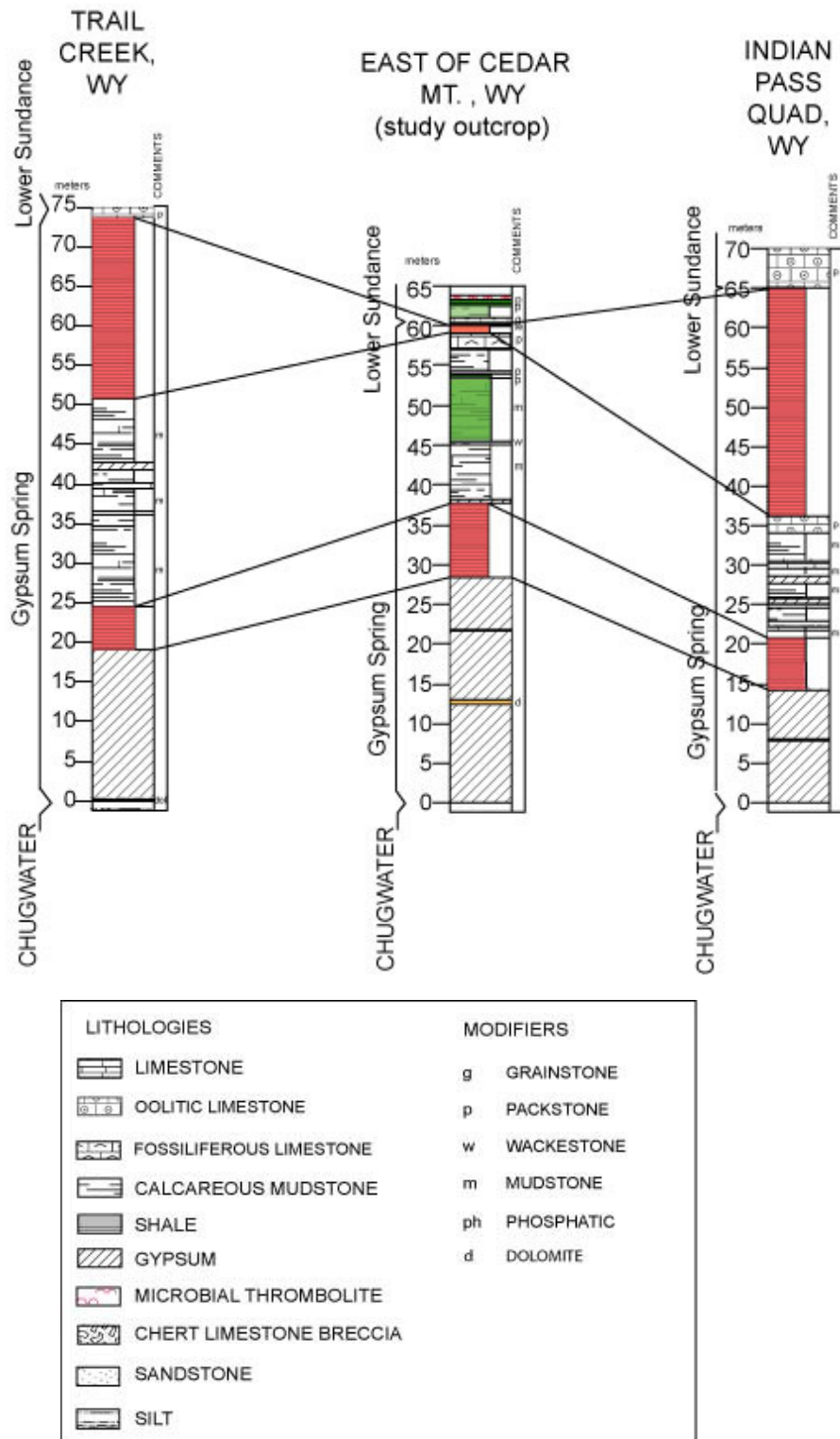


Figure 19: Stratigraphic cross-section from north to south across Cody area

(After Parcell, 2002)

must have been cut off by ancient weathering and erosion of water and/or wind which can be described by the missing part of the upper section. In addition, thrombolites of the Lower Sundance Formation appear to form nowhere else around the study area except for east of Cedar Mountain.

2) Lithology and Climatic Discussions

Gypsum Spring Formation: The existence of thick evaporite sequences within the Gypsum Spring Formation indicates at least seasonally arid and probably warm climate over an extended period. Topographic relief on a basin helps create a climate dry enough to form evaporites (Parrish, 1998). The lower gypsum and redbed unit of the Gypsum Spring Formation originated in a marine evaporitic basin that covered a widespread area extending from the Williston Basin on the north to the Twin Creek trough on the south. Restricted marine waters covered most of the Wyoming shelf area at this time, and numerous minor topographic basins were present when the initial invasion of the Gypsum Spring Sea occurred. This accounts for the considerably greater thickness of the lower gypsum in places (Peterson, 1957). The middle unit of the Gypsum Spring is represented by carbonate lithology. Shallow-water carbonates tend to be deposited in low latitudes, mostly less than 40° (Parrish, 1998). These carbonates indicate warm-water. Finally, the contact between the Gypsum Spring and Lower Sundance Formation is represented by oolitic grainstone. Ooids tend to form only in shallow (less than 2 m), agitated waters where daily wave and current activity is high (Handford and Loucks, 1993).

Lower Sundance Formation: According to Aitken (1967), thrombolites are suggested to develop in the subtidal zone, whereas the stromatolites develop in the intertidal zone. In many cases, the substrate of the thrombolites was a soft limy mud (Schmitt and Monninger, 1977). In the case of east of Cedar Mountain, the thrombolite also has a mudstone substrate (ECM MP9). The layers which cover the thrombolites are generally mudstone so there is no evidence of strong water energy during the deposits of thrombolites. In contrast, thrombolites from southeast Spain developed on the shelf edge where water turbulence caused irregular and uneven supplies of poorly sorted particulate sediment. Braga and Martin (1995) suggested that “these effects resulted in non-laminar accretion whose clotted appearance was further enhanced by physical damage in the high energy condition and by erosion”. Mancini et al (2004) suggested the initial growth of these thrombolites occurred when the rate of sea level rise began to slow and the amount of background sedimentation was low or zero.

The deposition of the Middle Jurassic microbial thrombolites occurred during the invasion of Sundance Sea when sea water started to decrease in water energy (maximum transgression). The marine transgression is marked by a basal shallow water oolitic grainstone and is overlain by highly fossiliferous carbonate sediments and followed by the deposition of microbial thrombolites. Extensive microbial growth occurred in response to the available accommodation space. As a result of low energy and low sedimentation rate, microbes and algae could easily grow on top of the sediments without much interruption. Furthermore, the relief and geographic location of the paleohighs seem to have had an effect on thrombolite growth and distribution at the study area, too. The microbial buildups were accumulated on a topographic high on the sea floor. The topography subsequently formed a trap for these organic compositions (Lehmann and Greenlee, 1993).

CHAPTER V

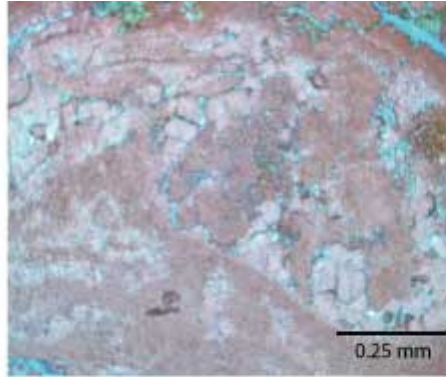
PETROGRAPHIC ANALYSIS

Rock samples from the microbial buildups were studied with both low power binocular scopes and petrographic scopes. Rock samples were collected from the outcrop and were studied initially with binocular scope. The overall characteristic of rock samples were described by Dunham's classifications (1962) and Munsell's soil color charts (2000). Dunham's (1962) classification is based solely upon depositional texture and considers two aspects of texture: (1) grain packing and the relative abundance of grains to micrite and (2) depositional binding of grains which means whether or not carbonate grains show evidence of having been bound together at that time of deposition (Boggs, 2001). A total of 13 thin sections from selected rock samples (from Lower Sundance) were prepared to study microcrystalline texture, mineralogy, micro-organisms, and so on. 8 thin sections came from the Lower Sundance Formation rock units beneath the microbial buildups, which are labeled as ECM MP1, ECM MP2, ECM MP3, ECM MP5, ECM MP6, ECM MP7, ECM MP8, and ECM MP9 from the bottom to the top, respectively. 5 thin sections of microbial buildup units, from the Lower Sundance Formation, are ECM S1 to ECM S5. All thin sections were carefully selected from the cutting rocks and gently polished. Furthermore, they were dyed in alizarin red to detect calcite. The detailed description of hand sample and thin section analysis is represented by Appendix B.

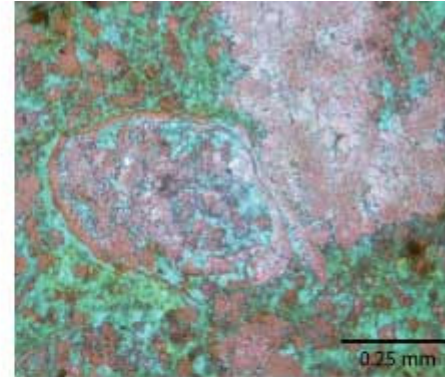
A. Sundance Microfacies of Lower Formation

1) Mudstone microfacies

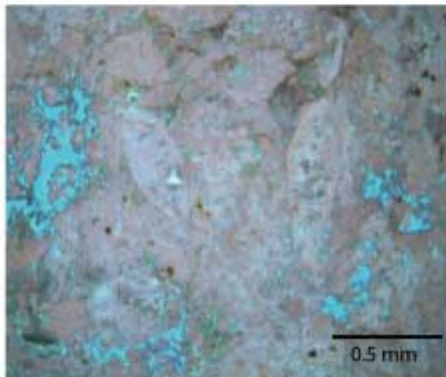
The first specimen is ECM MP6. This mudstone facies are found at the upper unit of the study section. This specimen contains ostracods (Figure 20) and some other type of microorganisms. The most dominant matrix is micrite matrix. This specimen is also found many fractures causing by weathering. This thin section came from the lower section of microbial thrombolite, so it has a similar clotted looking characteristic causing by microorganisms such as *Girvanella* and algae as in microbial thrombolite thin sections. The second specimen is ECM MP8. There are an abundance of ostracods in this specimen (Figure 20). This thin section specimen indicates highly dominance of ostracods with low diversity of other types of organisms.



ECM MP6a: micrite matrix with some sparry calcite



ECM MP6b: incomplete ostracod shell



ECM MP8b: micrite matrix with several ostracods



ECM MP8c: ostracods

Figure 20: Mudstone microfacies (part I) include ECM MP6 and ECM MP8 from Lower Sundance Formation at east of Cedar Mountain

The matrix is composed of micrite. There is iron oxide and many fractures in this specimen. The last specimen is ECM MP9. This mudstone is composed of skeletal grains of ostracods (Figure 21) and peloids. The matrix is dominantly micrite. There are some sparry calcites but very less. This sample also contains several fractures and clotted-looking features of *Girvanella*. *Leptocythere sp.* ostracods are found in this sample (Figure 21). Several burrows contain in this samples which can be seen easily from both binocular and microscopes.

2) Wackestone and packstone microfacies

Wackestones and packstones facies are commonly found in the lower section of the Lower Sundance Formation and also are found at the upper unit of the study section. ECM MP1 is a packstone at the base of the Lower Sundance Formation. This specimen is grain-supported packstone, with micrite matrix. The allochems contain ooids, subround to subangular in shape, and more than 30% of skeletal grains mostly ostracods (< 0.5 mm in size) and some pelecypods and foram. There are many types of organisms in this thin section, including pelecypods (*Homonya gallatinesis*), gastropods, foraminifera, bryozoan, coral fragments (~0.25 mm), ostracods *Cytherella sp.*, *Leptocythere sp.* and also algae such as *Solenopora* (Rhodophyta) and *Cayeuxia* (Chlorophyta) (Figure 22). Peloids are also commonly found in this specimen. The typical dominant mineral is calcite which can be easily seen by the red color of alizarin acid. ECM MP2 is a second thin section which is a packstone with micrite and some sparry calcite matrix. The allochems highly contain skeletal fragments and intraclasts and also consist of ooids and peloids. Most skeletal grains are ostracods, gastropods, and pelecypods (Figure 23). The intraclasts are long rectangular shape and about 1 mm. in diameter. Bryozoans (Figure 23) are also found in this thin section. Another wackestone and packstone microfacies is ECM MP5. It is a sandy dense wackestone to packstone or sandy carbonate. There are more than 10% of skeletal grains including pelecypods and ostracods fragments and peloids. The micrite matrix has been highly bioturbated with obvious burrows in thin section (Figure 24). Most mineralogy is calcite and quartz sands. The organisms are mostly ostracods and pelecypods. The last specimen is ECM MP7. This is a dense wackestone to packstone. The allochems contain skeletal grains of microorganisms such as foraminiferous, pelecypods, and ostracods (Figure 24) and peloids.

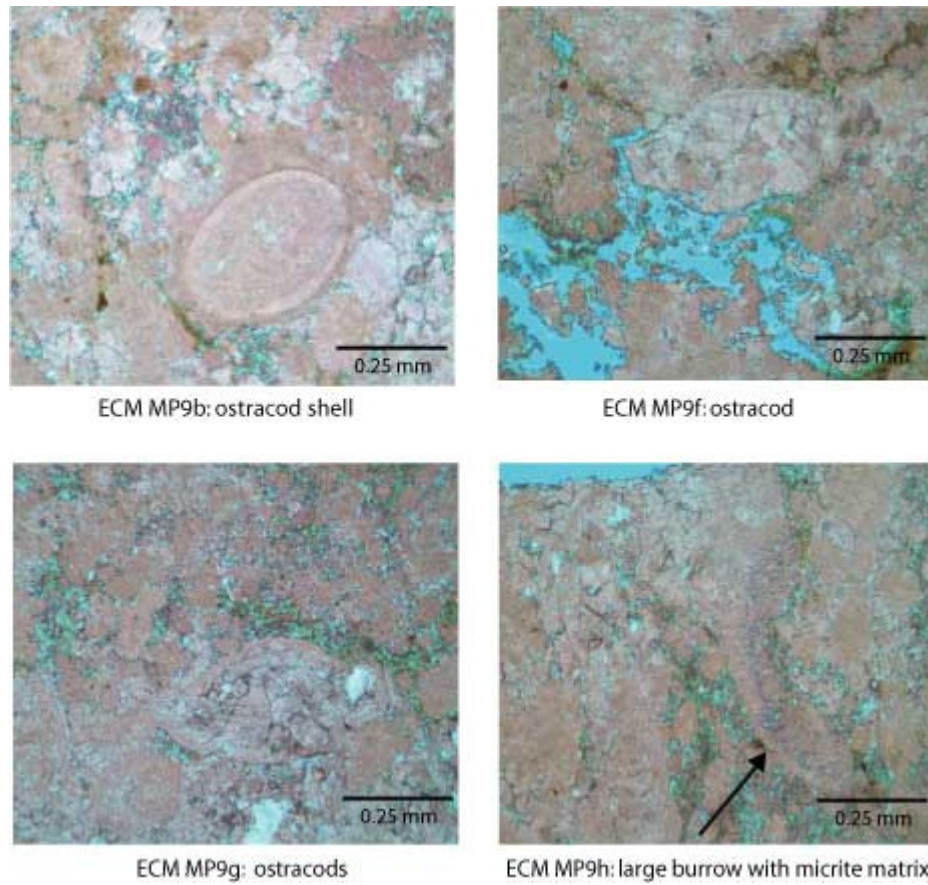
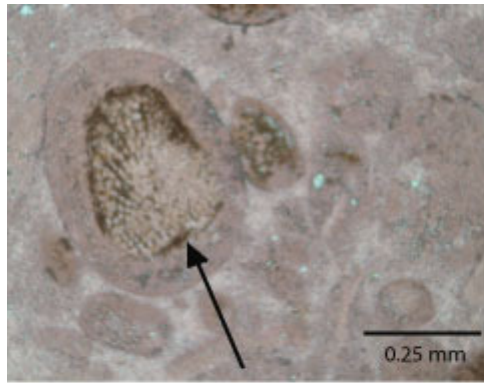
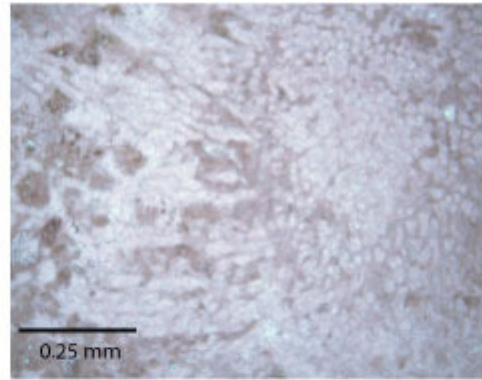


Figure 21: Mudstone microfacies (part II) include ECM MP9 from Lower Sundance Formation at east of Cedar Mountain



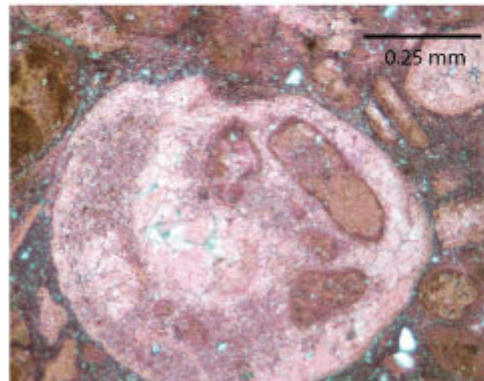
ECM MP1d: Cayeuxia (Chlorophyta algae)



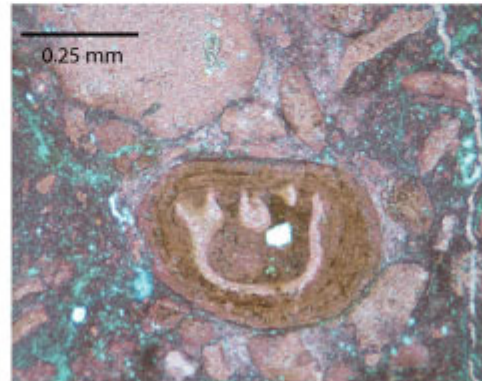
ECM MP1: Solenopora (Rhodophyta algae)



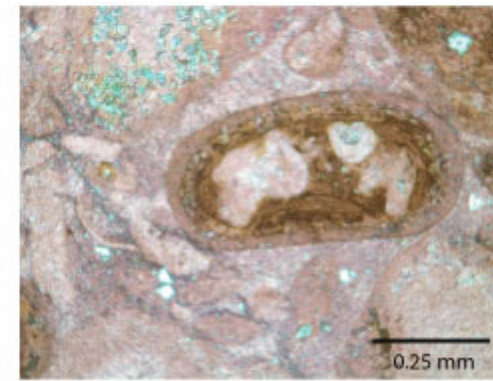
ECM MP1: pelecypod shell fragments



ECM MP1h: Foraminifera



ECM MP1i: ostracod (Leptocythere sp.)

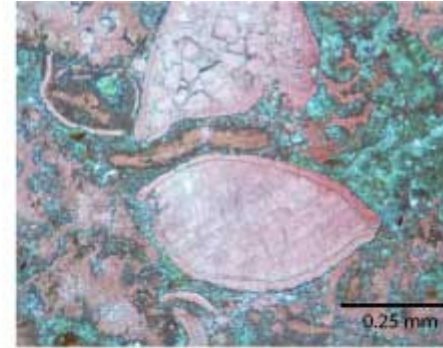


ECM MP1j: ostracod

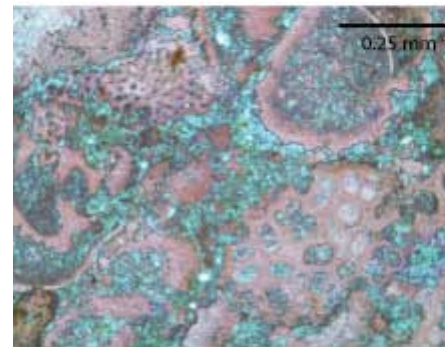
Figure 22: Packstone microfacies (part I: ECM MP1) from Lower Sundance Formation at east of Cedar Mountain



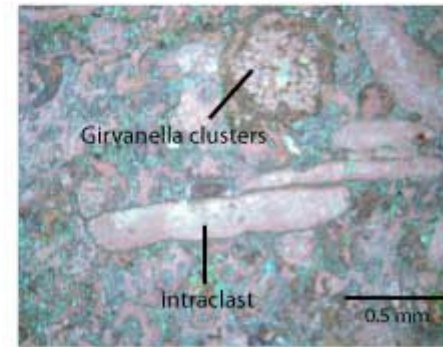
ECM MP2a: Gastropod



ECM MP2b: oyster filled with sparry calcite

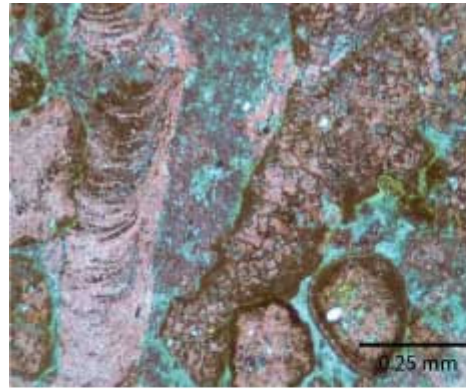


ECM MP2c: Bryozoan and skeletal grains

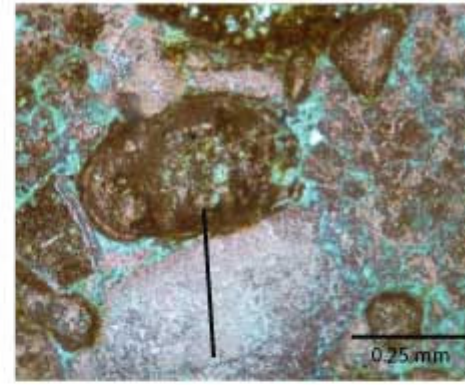


ECM MP2e: Girvanella and intraclasts

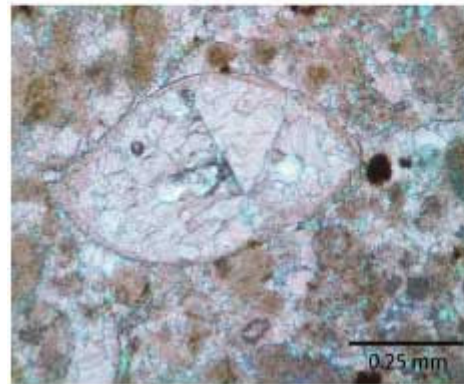
Figure 23: Packstone microfacies (part II: ECM MP2) from Lower Sundance Formation at east of Cedar Mountain



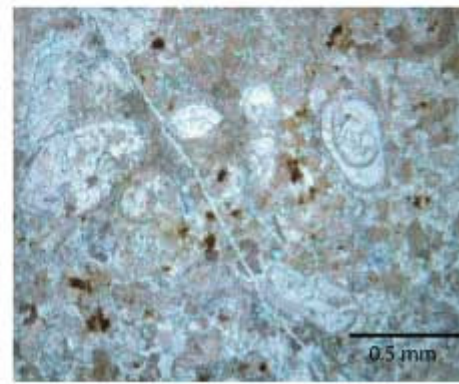
ECM MP5b: burrow trace



ECM MP5e: ostracod shell



ECM MP7a: ostracod filled with sparry calcite



ECM MP7c: skeletal grains in micrite matrix

Figure 24: Wackestone and Packstone microfacies (part III: ECM MP5 and ECM MP7)
from Lower Sundance Formation at east of Cedar Mountain

The matrix is composed of both micrite and sparry calcite with iron oxide and pyrite which indicate the reducing condition. The mineralogy is composed of calcite, pyrite and iron oxide. Thin section specimens of this facies show highly dominant type of organisms such as ostracods with low diversity of others. There are not many fossils of pelecypods or gastropods as fossils of ostracods.

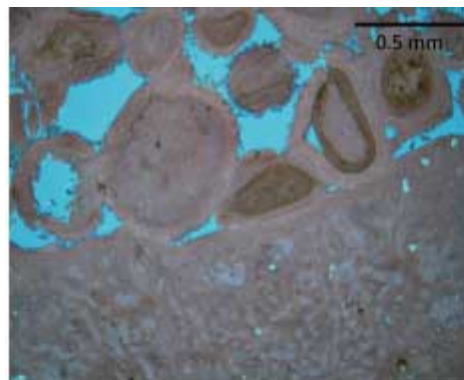
3) Grainstone microfacies

The oolitic grainstone (ECM MP3) contains more than 50% of rounded to subrounded ooids including both circular and elongate shape (Figure 25). These ooids have a size around 1 mm. and less. There are some skeletal grains of ostracods and pelecypod shell fragments including bryozoans' fragments and *Solenopora* algae in this specimen. Some of these ooids nucleus made from skeletal grains and some made from cyanobacteria such as *Girvanella*. This thin section has a very high porosity with very less in micrite matrix. The ooid grains are touching each others and are connected by the sparry calcite cement. Both matrix and ooids are dyed by red color of alizarin acid.

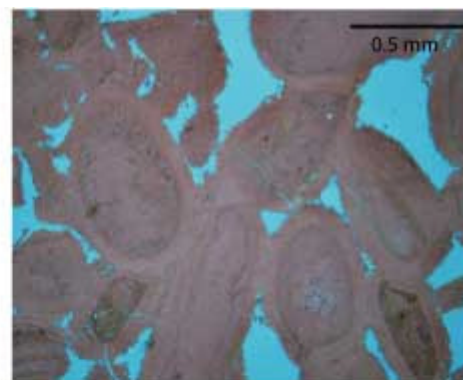
4) Microbial thrombolite microfacies

All the samples from ECM S1 to ECM S5 came from microbial thrombolites lithology. The organisms that responsible for the formation of these microbial carbonates are mostly microscopic size. According to Dunham's classification (1962), "the autochthonous limestone that original components organically bound during the deposition should called boundstone". Boundstone that encrust and bind by organisms called "bindstone" (Dunham, 1962). But in this study, the specific name of the microbial carbonate is called thrombolite. Thrombolites are clotted fabric and their distinctive difference allows them to be readily distinguished in the field and also in hand-specimen. Most of microbialite specimens have a relatively high porosity and contain many fractures.

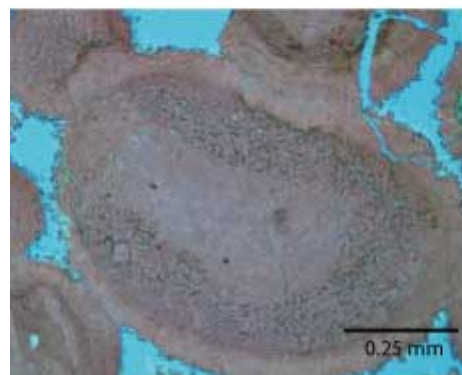
First specimen is ECM S1. This sample is composed of intraclasts, with some peloids, ostracods and *Girvanella* (Figure 26). The backgrounds mostly are micrite matrix with some sparry calcite cement. There are also several algae in this sample. These algae are elongate in shape and consist of septa inside some of them are filled in with sparry calcite. ECM S2 sample is similar to ECM S1 except for the ECM S2 does not have much peloids; however, there are more algae in this sample than ECM S1. The algae are composed of septa inside and are filled with sparry calcite.



ECM MP3a: Ooids



ECM MP3b: subrounded ooids with high porosity



ECM MP3d: Girvanella is a nucleus within ooid



ECM MP3e: ooids with sparry calcite matrix

Figure 25: Grainstone microfacies (ECM MP3) from Lower Sundance Formation at east of Cedar Mountain

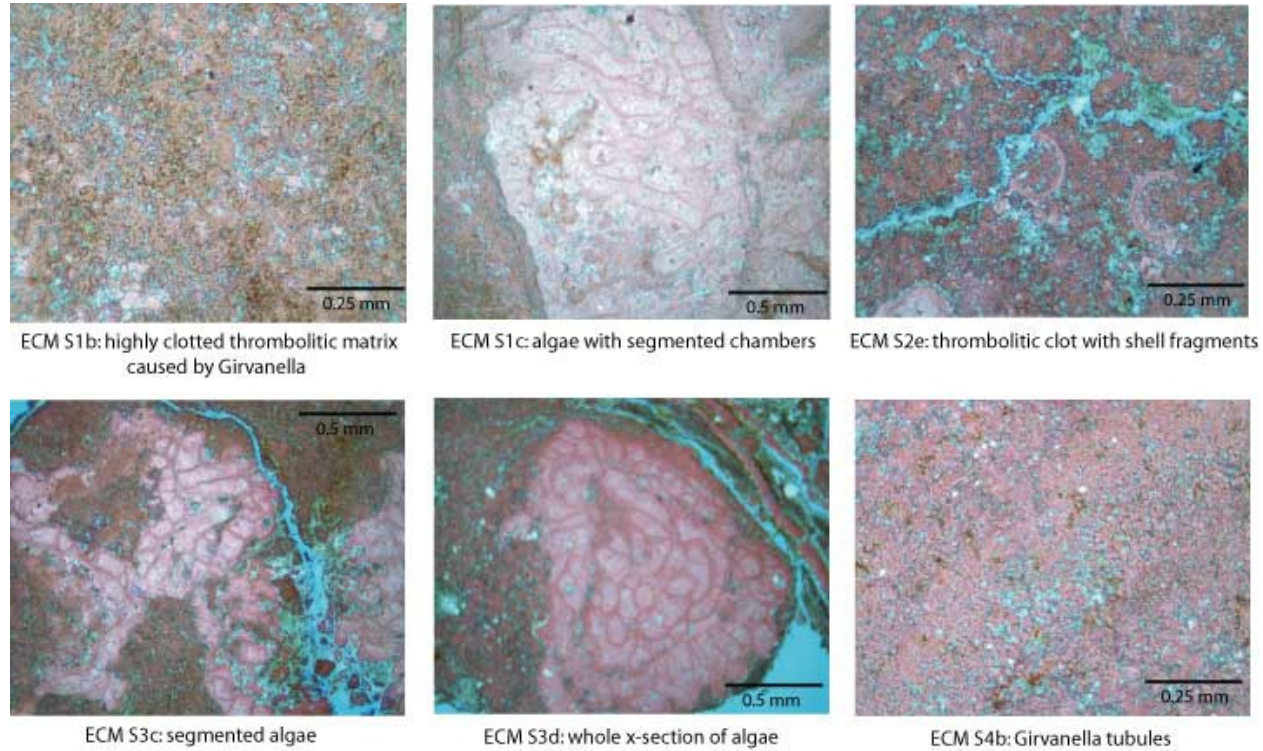
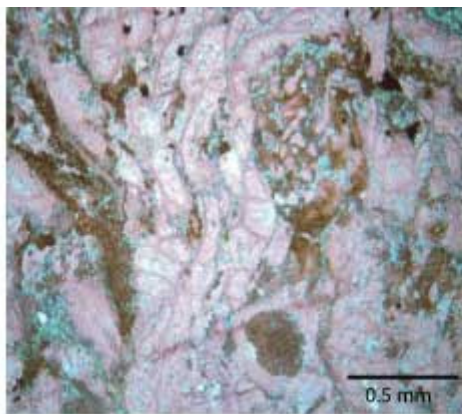
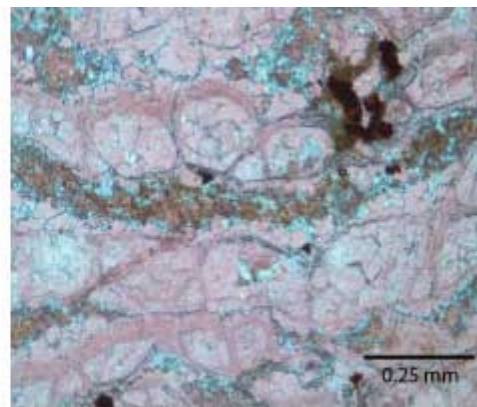


Figure 26: Microbial thrombolite microfacies (part I) from Lower Sundance Formation at east of Cedar Mountain

Girvanella is dominant in this specimen. This thin section represents by the brownish color of iron oxide which indicates later diagenetic condition. ECM S3 specimen has many fractures and contains large crystalline algae. The matrix is mostly micrite, with highly clotted-looking features. According to thin section, some areas contain cross-section of the algae which have several tubules of possibly *Girvanella*. ECM S4 sample was taken from the whole thrombolite head. The entire matrix is micrite with coated grains. Several segmented algae and *Girvanella* are found in this thin section with clotted looking character. This specimen does not have many fractures but still indicates the sign of reducing environment from brownish color of iron oxide. ECM S5 is also composed of thrombotic clotted features. There are several segmented algae (Figure 27) inside this thin section. The matrix is micrite with some brownish color of iron oxide.



ECM S5a: segmented algae filled with sparry calcite



ECM S5d: close up algae with segments

Figure 27: Microbial thrombolite microfacies (part II) from Lower Sundance Formation
at east of Cedar Mountain

B. Discussion of Allochems and Fossils

1) Ostracods

Deckker et al (1988) suggested that “ostracods have colonized nearly every type of aquatic environment from fresh to marine to hypersaline and even phreatic waters”. Ostracods can be used to reconstruct palaeoenvironments dating as far back as the Cambrian (Deckker, 1988). Ostracods are known to be very useful in the paleoecological analysis of marginal marine deposits, which are generally poorly represented by other fossil groups (Mette, 1997). Colin (1988) also states a very likely concept that “ostracods are amongst the best microfossils for palaeoenvironmental interpretations.

Most of carbonate rocks (wackestone to packstone) at the base of the Lower Sundance Formation are highly fossiliferous and include ostracods, gastropods, and pelecypods. Early work by Swain and Peterson (1952) on ostracods of the Sundance Formation resulted in identification of 16 species of ostracods. Taxonomic problems exist with some generic assignments by Swain and Peterson (1952) when compared to generic assignments in the ostracod Treatise (Moore, 1961). For example, *Macrocypris* was identified in the unit by Swain and Peterson (1952). The Treatise assigns this genus to the Tertiary Period only (Moore, 1961:Q207). In each case that an ostracod genus was identifiable in thin section from the study area, Treatise classification was used for identification purposes.

Two genera of ostracods *Cytherella* (=Cytherelloidea?) and *Leptocythere* (Figure 22) were identified in thin sections of packstones from the study area. Although both genera belong to the filter-feeding platycopids which have a survival advantage in times of reduced oxygen (Whatley, 1995; Schudack, 1999), each occupies a different niche. The distribution of *Cytherella* (=Cytherelloidea?) is bounded in the oceanic zone to mean water temperature that exceeds 10° C, has been interpreted as an indicator for relatively warm water temperatures (Schudack, 1999). Modern, living members of the genus *Leptocythere* live in a range of salinities and temperatures (Teeter, 1975). Packstones that contain these ostracods are interpreted as originating in warm water environments.

2) Ooids

Ooids, from oolitic grainstone thin section (ECM MP3), are subrounded to rounded in shape and grain-supported with very less micrite matrix. These ooids must have formed where there are strong bottom currents with agitated-water conditions exist and where the saturation levels of calcium bicarbonate are high (Boggs, 2001). The high energy of water wash away micrite matrix that used to be in the section when it was deposited. After, the micrite matrixes were was away, it left out with high porosity. Then the sparry calcite were deposited or filled in these porosities over the time. Precipitation of ancient calcitic ooids appears to have been particularly important during the Middle Paleozoic and the Middle Mesozoic time (Boggs, 2001).

3) Algae

Algae and microbes are another type of organisms within these thin section specimens of the study section. They are containing from the bottom (ECM MP1) to the top of the unit (ECM S5). There are several types of algae in the Lower Sundance Formation specimens including Rhodophyta and Chlorophyta in wackestone and packstone thin section. Generally, most of algae inhabit in normal marine environment including the following types of algae. See Appendix C for algae classification and description.

3.1) *Solenopora* (Figure 22) is a genus of Rhodophyta which is characterized by their tubular filaments forming fan-shaped masses (Riding, 1985). During the Mesozoic, Solenoporaceae became more important, particularly during the Jurassic period (Johnson, 1961). They appear to have attained their greatest size and probably the greatest number of individuals during this time (Johnson, 1961). The environmental distribution of the Solenoporaceae is comparable to some modern coralline algae, but this group was not as varying in its depth and temperature ranges as the Corallinaceae (Johnson, 1961).

3.2) *Cayeuxia* is another type of algae that is found in the samples (Figure 22). Johnson (1961) classified this genus into Chlorophyta, whereas Wray (1977) put into Cyanophyta. *Cayeuxia* have rounded tufts or cushions plants forms. The tufts consist of a mass of loosely-packed, radially-arranged, branching tubular filaments (Johnson, 1961). *Cayeuxia* have a right-angle branching pattern (Wray, 1977), this type of branching characterizes *Cayeuxia* genus.

4) Cyanobacteria

Girvanella: Many thin section specimens (ECM MP3, ECM MP9, ECM S1, S2, S3, S4, and S5) include *Girvanella*. *Girvanella* is a type Cyanobacteria that made all the specimens have clotted-looking features. By their morphology, Riding (1985) placed this genus into tubiform with tangled and coiled tubes. He described the characteristic of *Girvanella* as “loosely tangled tubes with non-radial, non-fanlike arrangement of tubes and virtual absence of branching”. Wray (1977) suggested that “*Girvanella* usually form loosely and occur in groups”. They tend to twisted together to form nodules and encrusting masses as seen in thin section specimen of ECM MP3. The *Girvanella* is often used as a nucleus of ooids (Figure 25). *Girvanella* has been reported most often from marine environments, generally in shallow shelf, carbonate facies (less than 50 m), although it has been recorded in nonmarine limestones too (Wray, 1977). Wray (1977) suggested that this type of alga could not used to discriminate marine from non-marine facies because they occurs in a variety of non-marine and shallow marine environments.

In general, microbialites may contain a variety of internal structures, whereas in this study the microbial crust specimens (ECM S1 to S5) show primarily a clotted mesostructure characteristic of thrombolites. A thrombolite is defined as microbial structure characterized by a mesoscopic clotted internal fabric (Mancini, et al, 2004). Thrombolites or organosedimentary structures are produced by sediment trapping, binding and/or precipitation as a result of the growth and metabolic activity of microorganisms, principally cyanophytes (Burne and Moore, 1987). The thrombolitic features in each specimen were not only influenced by the algae but also controlled by microbes that build them. All of the studied microbial specimens have relatively similar features. They have clotted-looking or thrombolitic characters which are mainly built by *Girvanella* mat and other microbes. Cyanobacteria are one type of microbes that lives within microbial thrombolites (Parcell, 2004). Cyanobacteria filaments perform such a good trap for fine grained sediments. Their filaments produce gelatinous sheet which is sticky and make the sediment trap to them. When sediments cover all over these cyanobacteria, they grow another layer of filaments through and over the sediments, so they can continue to photosynthesize. Then another layer of sediment is trapped which building up the layer of organic-rich over another layer of sediments-rich.

CHAPTER VI

ISOTOPIC ANALYSIS

The stable isotopes of oxygen and carbon are important indicators of paleoclimate studies and the analysis and interpretations of these isotopes has become almost routine (Parrish, 1998). Stable isotope data provide information about paleotemperature, paleoprecipitation, and paleoevaporation, and also production, burial and weathering of organic carbon. Stratigraphic variation in the carbon isotopic ($\delta^{13}\text{C}$) value of marine carbonate and organic matter preserved within it has become a popular tool for supporting paleoclimatic hypotheses and refining stratigraphic correlation (Ripperdan, 2001).

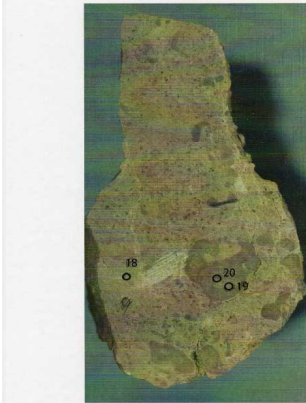
Bartolini (2003) suggested that “carbon and oxygen isotopes are commonly used to trace paleoceanographic and paleoclimatic changes”. The oxygen isotopic composition of carbonates is used as paleotemperatures or as tracer of seawater isotopic composition (e.g., palaeosalinity) although diagenesis often drastically affects the primary signature of $\delta^{18}\text{O}$ (Bartolini, 2003; Scholle and Arthur, 1980). Scholle and Arthur, (1980) also used carbon isotope data in studies of paleosalinity and early diagenesis. Negative and positive $\delta^{13}\text{C}$ variations are interpreted in terms of carbon cycle perturbations, primary productivity changes, burial rate of organic matter, CO_2 variations in the atmosphere (Bartolini, 2003).

In this thesis, carbon and oxygen stable isotope were examined from the Lower Sundance Formation rocks at the study section and PDB was used as a reference. Samples (Figure 28 and 29) were selected from the carbonate rocks including mudstone, wackestone, packstone, grainstone and microbial thrombolite of the Lower Sundance Formation sections. Rock powder samples were run through a Thermo Finnigan MAT 253 mass spectrometer (Figure 5) and obtaining the isotopic values of carbon and oxygen as indicated in table 2. All the data and conclusions that are derived from oxygen and carbon isotopes must be considered with caution. All samples had multiple sampling points taken to compare isotope values.

Isotopic sample: all these samples have an average size of about 4-5 cm

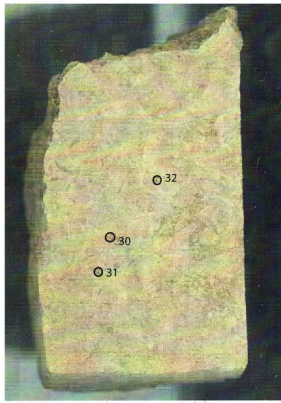
ECM_MP1: packstone

ECM_MP1.18: peloidal packstone matrix
ECM_MP1.19: microbe mudstone
ECM_MP1.20: microbe mudstone
ECM_MP1.21: microbe mudstone



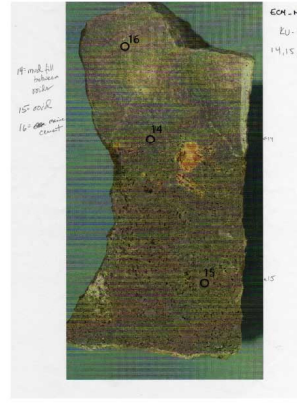
ECM_MP2: wackestone to packstone

ECM_MP2.30: peloidal matrix
ECM_MP2.31: spar cement
ECM_MP2.32: microbial buildup
ECM_MP2.33: microbial buildup



ECM_MP3: packstone to grainstone

ECM_MP3.14: mud fill between ooids
ECM_MP3.15: ooids
ECM_MP3.16: marine cement



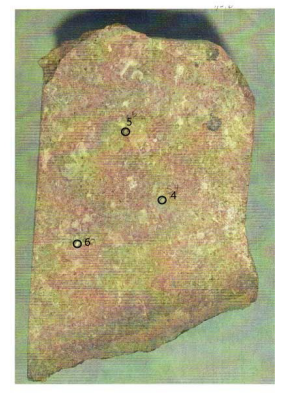
ECM_MP4: mudstone

ECM_MP4.17: mudstone



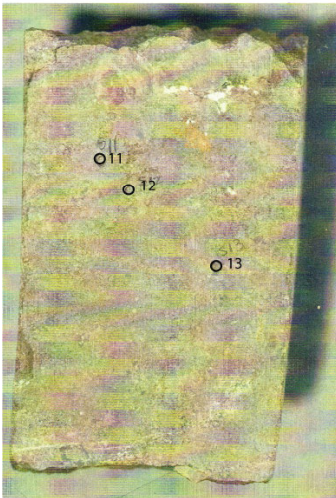
ECM_MP5: packstone

ECM_MP5.4: micrite
ECM_MP5.5: fossil spar
ECM_MP5.6: spar cement



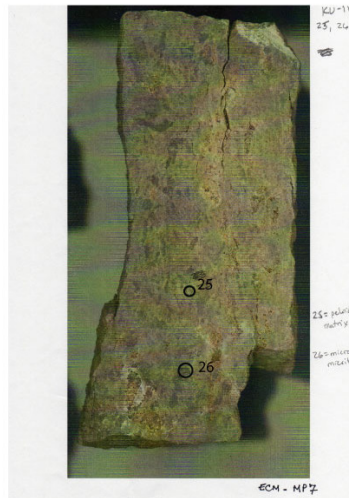
ECM_MP6: laminated wackestone

ECM_MP6.11: microbe mudstone
ECM_MP6.12: peloidal wackestone
ECM_MP6.13: micrite



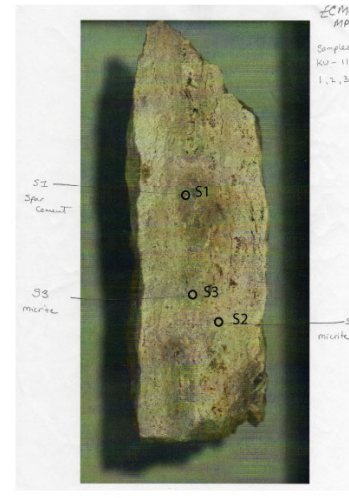
ECM_MP7: wackestone to packstone

ECM_MP7.25: peloidal matrix
ECM_MP7.26: microbe micrite



ECM_MP8: packstone

ECM_MP8.1: spar cement
ECM_MP8.2: micrite
ECM_MP8.3: micrite



ECM_MP9: mudstone

ECM_MP9.3: microbe mudstone (dark)
ECM_MP9.4: microbe mudstone (light, partly recrystal)
ECM_MP9.5: recrystal microbialite



Figure 28: Selected spots from selected rock sample (ECM MP1 to ECM MP9) that used for run the isotopic composition.

ECM_S1: microbial thrombolite
ECM_S1.2: microbialite



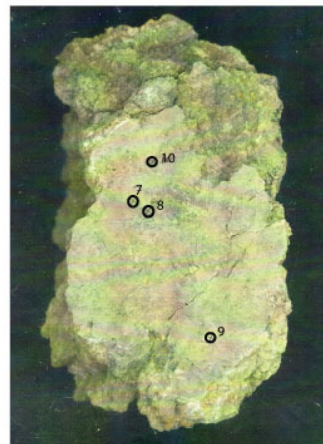
ECM_S2: microbial thrombolite
ECM_S2.14: microbe (center)
ECM_S2.15: microbe (edge)
ECM_S2.16: microbe
ECM_S2.17: glauconite matrix



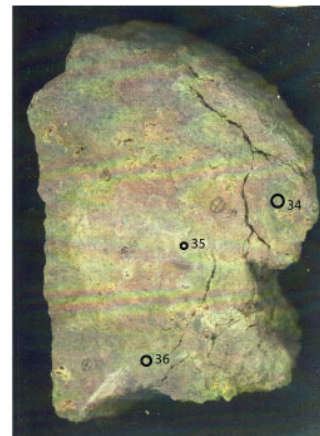
ECM_S3: microbial thrombolite
ECM_S3.18: microbe mud
ECM_S3.19: microbe mud
ECM_S3.20: glauconite matrix



ECM_S4: microbial thrombolite
ECM_S4.7: micrite mud
ECM_S4.8: micrite mud
ECM_S4.9: micrite mud
ECM_S4.10: interstitial material
between microbialite



ECM_S5: microbial thrombolite
ECM_S5.34: microbe micrite
ECM_S5.35: microbe micrite
ECM_S5.36: microbe micrite
ECM_S5.37: spar



ECM_BM: belemnite
ECM_BM22: belemnite
ECM_BM23: belemnite
ECM_BM24: belemnite



Figure 29: Selected spots from selected rock sample (ECM S1 to ECM S5) that use for run isotopic analysis.

Table 2: Stable Isotopic Composition Values of Carbon and Oxygen

			$\delta^{13}\text{C}$ (‰)	SE ($\delta^{13}\text{C}$)	$\delta^{18}\text{O}$ (‰)	SE ($\delta^{18}\text{O}$)
ECM_MP1	ECM_MP1.18	peloids	2.44	0.041	-6.71	0.071
packstone	ECM_MP1.19	microbe mudstone	2.54	0.033	-7.61	0.044
	ECM_MP1.20	microbe mudstone	2.45	0.065	-8.04	0.055
	ECM_MP1.21	microbe mudstone	3.10	0.052	-6.82	0.046
ECM_MP2	ECM_MP2.30	peloidal matrix	1.91	0.048	-8.08	0.054
wackestone to packstone	ECM_MP2.31	spar	2.10	0.044	-8.54	0.070
	ECM_MP2.32	microbial buildup	2.17	0.043	-8.25	0.045
	ECM_MP2.33	microbial buildup	2.08	0.052	-8.41	0.070
ECM_MP3	ECM_MP3.14	mud fill btw ooids	1.51	0.043	-9.96	0.083
packstone to grainstone	ECM_MP3.15	ooids	1.91	0.036	-5.76	0.078
	ECM_MP3.16	spar	2.41	0.034	-8.09	0.066
ECM_MP4	mudstone	no sample				
ECM_MP5	ECM_MP5.4	micrite	2.27	0.026	-6.93	0.060
packstone	ECM_MP5.5	spar	2.15	0.030	-6.95	0.077
	ECM_MP5.6	spar	2.27	0.036	-6.79	0.072
ECM_MP6	ECM_MP6.11	microbe mudstone	1.46	0.036	-6.69	0.087
laminate mudstone	ECM_MP6.12	peloidal mudstone	1.62	0.045	-6.59	0.068
	ECM_MP6.13	micrite	2.07	0.046	-6.38	0.095
ECM_MP7	ECM_MP7.25	peloidal matrix	1.84	0.025	-8.15	0.064
wackestone to packstone	ECM_MP7.26	microbe micrite	1.46	0.038	-9.35	0.068
ECM_MP8	ECM_MP8.3	micrite	0.93	0.074	-8.52	0.132
ECM_MP9	ECM_MP9.3	microbe mudstone (dark)	1.85	0.042	-7.39	0.08
mudstone (substrate)	ECM_MP9.4	microbe mudstone (light; partly recrystal)	2.22	0.041	-6.57	0.047
	ECM_MP9.5	recrystal microbialite	1.71	0.044	-7.69	0.043
ECM_S1	ECM_S1.2	microbialite	2.52	0.025	-5.95	0.065
ECM_S2	ECM_S2.14	microbialite (center)	1.66	0.054	-8.36	0.073
microbial thrombolite	ECM_S2.15	microbialite (edge)	1.89	0.042	-7.24	0.051
	ECM_S2.16	microbialite	2.05	0.032	-7.14	0.044
	ECM_S2.17	glauconite matrix	2.14	0.049	-6.31	0.066
ECM_S3	ECM_S3.18	microbe mud	1.92	0.036	-5.78	0.073
microbial thrombolite	ECM_S3.19	microbe mud	2.24	0.027	-5.89	0.037
ECM_S4	ECM_S4.7	micrite (center)	2.22	0.019	-5.91	0.028
microbial thrombolite	ECM_S4.8	micrite (edge)	2.44	0.048	-6.19	0.02

Table 2: Stable Isotopic Composition Values of Carbon and Oxygen

		$\delta^{13}\text{C}$ (‰)	SE ($\delta^{13}\text{C}$)	$\delta^{18}\text{O}$ (‰)	SE ($\delta^{18}\text{O}$)	
	ECM_S4.9	micrite (center)	2.35	0.034	-6.13	0.048
	ECM_S4.10	interstitial material btw microbialite	1.98	0.059	-6.73	0.054
ECM_MP2	ECM_MP1.22	peloids	1.92	0.038	-6.41	0.055
packstone	ECM_MP1.23	microbe mudstone	1.91	0.038	-6.36	0.054
	ECM_MP1.24	microbe mudstone	1.91	0.038	-6.31	0.054
	ECM_MP1.25	microbe mudstone	1.90	0.038	-6.27	0.053
ECM_MP3	ECM_MP2.34	peloidal matrix	1.89	0.038	-6.22	0.053
wackestone to packstone	ECM_MP2.35	spar	1.88	0.037	-6.17	0.053
	ECM_MP2.36	microbial buildup	1.88	0.037	-6.13	0.052
	ECM_MP2.37	microbial buildup	1.87	0.037	-6.08	0.052

A. Result of Carbon and Oxygen Stable Isotope

The isotopic composition values of belemnites can be used as a proxy for chemical composition of marine water because belemnites did not fractionate sea water, i.e., actively select specific isotopes, during shell formation. In addition, belemnites are composed of low-magnesium calcite that results in a chemically stable shell through time. As a result, belemnite calcite constitutes the best standard for the geochemistry of Jurassic seawater (Rosales, 2005), and provide a reasonable approximation of sea water chemistry during deposition of a rock unit. In the Sundance Formation, three samples of a belemnite from the green-shale facies above the thrombolite unit were selected for isotopic analysis. All isotopes from lower in the section will be compared to the known belemnite isotopic composition for environmental interpretation.

Results of isotopic analyses indicate that all $\delta^{13}\text{C}$ and $\delta^{18}\text{O}$ isotopes from the Lower Sundance Formation are more negative than the isotopic composition of the belemnite. According to isotopic data of carbon and oxygen stable isotopes (table 2 and figure 30), carbon isotopic values of belemnite are 2.11‰ to 2.54 ‰ and oxygen isotopic values are -2.34 ‰ to -2.36 ‰. Most of carbonate samples from wackestone (ECM_MP1) at the lower unit to mudstone (ECM_MP9) at the upper unit have carbon isotopic values between 1.5 ‰ to about 2.5 ‰ and oxygen isotopic values of about -6 ‰ to -9 ‰. Microbial thrombolite samples (ECM_S1 to ECM_S5) have carbon isotopic values between 1.5 ‰ to 2.5 ‰ and oxygen isotopic values between -5.5 ‰ to -9 ‰ (table 2 and figure 30). The plot of the Middle Jurassic (Lower Sundance Formation) carbon and oxygen isotopic values is represented on figure 30. Both carbon and oxygen isotopic values of rock samples tend to cluster together within relatively close range of negative values trend.

The carbon and oxygen isotopic values from samples within the Lower Sundance Formation were plotted against time (Figure 31). When isotopic values are plotted against geologic time, all $\delta^{13}\text{C}$ and $\delta^{18}\text{O}$ isotopic values are more negative than the stratigraphically higher belemnite (figure 31). Carbon isotopic values of wackestone and packstone at the bottom unit (Figure 31: unit #1) of the study section are 1.9 ‰ to 3.1 ‰, and oxygen isotopic values are -6.7 ‰ to -8.5 ‰. The carbon isotopic values of this wackestone and packstone unit have values that are relatively close to the carbon isotopic composition of the belemnite, but somewhat more negative than those of belemnite.

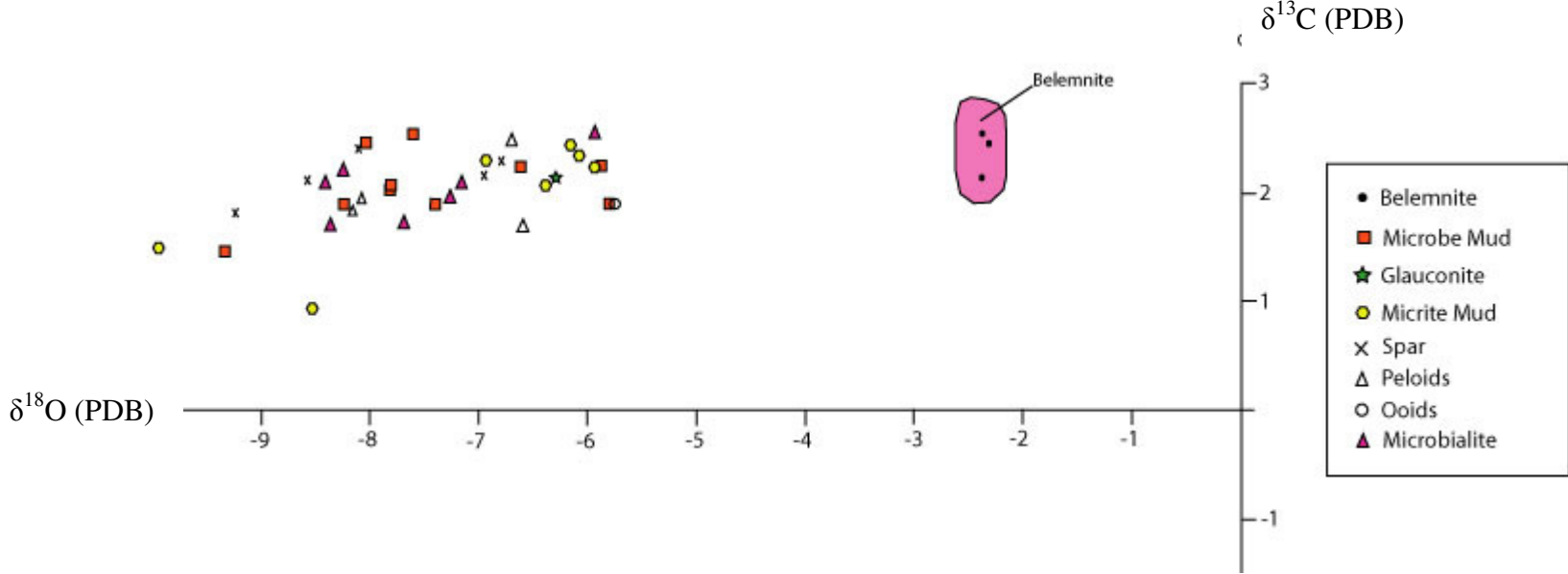


Figure 30: Carbon and oxygen isotopic values from Middle Jurassic section (Lower Sundance Formation), Bighorn Basin, WY

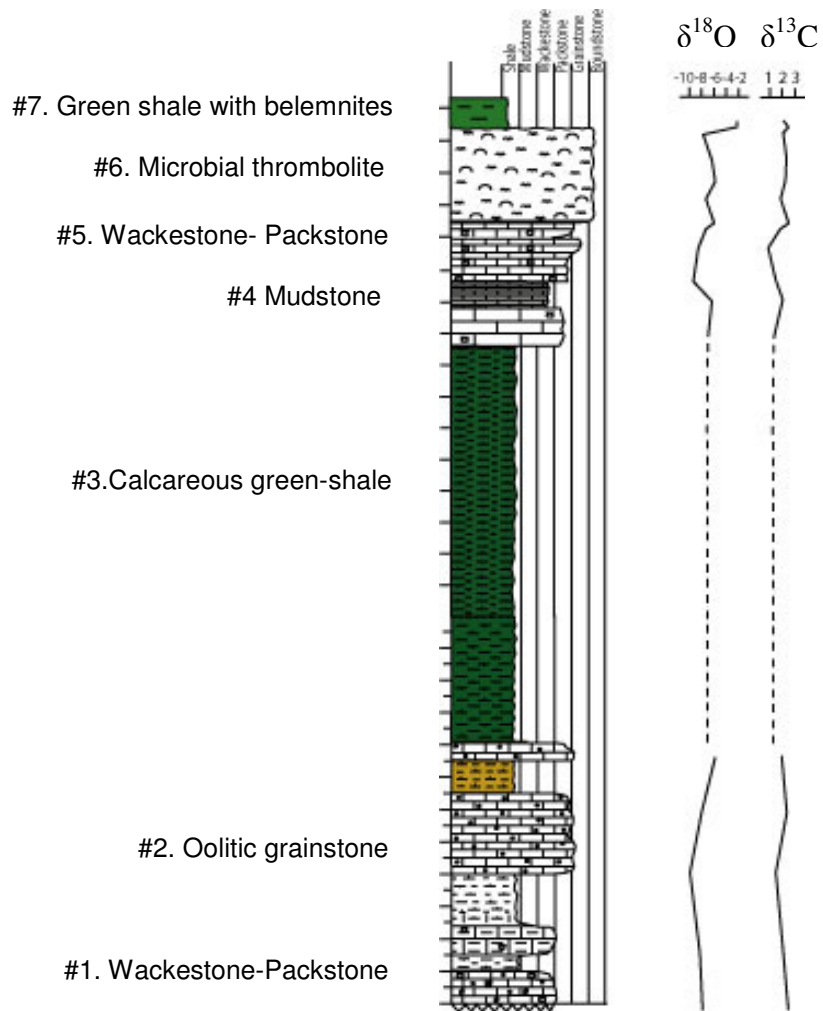


Figure 31: Carbon and oxygen isotopic composition curve compare to stratigraphy of Lower Sundance Formation

The oxygen isotopic values of this unit have more negative values than the oxygen isotopic values of belemnite. The carbon isotopic values of oolitic grainstone (Figure 31: unit #2) are 1.5 ‰ to 2.4 ‰, and oxygen isotopic values are -5.7‰ to -9.9 ‰. Both carbon and oxygen isotopic values from this unit are much more negative values than carbon and oxygen isotopic values of belemnite. There is no isotopic data from calcareous green shale (Figure 31: unit #3) of the middle unit from the study section. The carbon isotopic values of mudstone (Figure 31: unit #4) are 1.4 ‰ to 1.6 ‰, and oxygen isotopic values are -6.6 ‰ to -6.7 ‰. Both carbon and oxygen isotopic values from this mudstone unit are also more negative values than carbon and oxygen isotopic values of belemnite. The carbon isotopic values of wackestone and packstone (Figure 31: unit #5) at the upper unit of the Lower Sundance Formation section are 0.9 ‰ to 1.8 ‰, and oxygen isotopic values are -8.5 ‰ to -9.3 ‰. Both carbon and oxygen isotopic values from this unit are more negative than carbon and oxygen isotopic values of belemnite. The carbon isotopic values of microbial thrombolite unit (Figure 31: unit #6) at the uppermost of the study section are 1.6 ‰ to 2.5 ‰, and oxygen isotopic values are -5.7 ‰ to -9.2 ‰. Most of carbon isotopic values of microbial thrombolite unit are relatively close to carbon isotopic values of belemnite, but some are slightly negative than those of belemnite. The oxygen isotopic values of microbial thrombolite unit are much more negative than the oxygen isotopic values of belemnite. Both oxygen and carbon isotopic curves fluctuate upsection (Figure 31). Overall the trend of both isotopic signatures is toward negative when compared to belemnite at top of stratigraphic unit.

In addition, all carbon and oxygen isotopic values of microbial thrombolites from the Late Bathonian to Early Callovian, Wyoming are not similar to the values of microbial crusts from the Oxfordian and Kimmeridgian of Europe. Carbon and oxygen stable isotopic composition values of microbial crusts of the Oxfordian and Kimmeridgian reefs (Leinfelder, 1993) from Europe is represented in figure 32. Leinfelder has been studied carbon and oxygen isotope values of microbial crusts from Spain, Portugal, and Germany. The carbon isotopic values of microbial crusts from Europe are -1.5 ‰ to 2.5 ‰, with mostly $\delta^{13}\text{C}$ values are positive between 0 to 2.5 ‰ which slightly differ from carbon isotopic values of microbial thrombolite from Wyoming. The oxygen isotopic values of microbial crusts from Europe are -1 ‰ to -5.5 ‰. The comparison between these two locations (Wyoming and Europe) shows a dissimilar trend of carbon and oxygen isotopic values. The oxygen isotopic data of microbial thrombolite seem to

shift toward more negative values which is describe as becoming lighter (Schidlowski, 2000) or depleted in ^{18}O (enriched in ^{16}O).

Based on the isotopic data of both carbon and oxygen from rock samples of the study sections that were plotted (Figure 30) and compared horizontally to the carbon and oxygen isotopic values of belemnite, both carbon and oxygen isotopic values are shift toward negative values. Furthermore, the isotopic data were also plotted against the stratigraphic column of the Middle Jurassic Lower Sundance Formation section (Figure 31). This figure indicates both carbon and oxygen isotopic curves are more negative than both isotopic composition values of belemnite. In addition, the carbon and oxygen isotopic values of microbial crusts from Wyoming show a different trend from those of Europe. The fact that all isotopic values of carbonate rocks from the Lower Sundance Formation of the study section are more negative than the standard for seawater as indicated by the belemnite isotopic values probably indicates that the entire stratigraphic column has been altered post-depositionally by meteoric water. $\delta^{18}\text{O}$ values are sensitive to post-depositional diagenetic processes (Ripperdan, 2001) so these values can provide insight into the diagenetic history of a sample. The oxygen isotopic values of all samples have slightly more negative values compare to that of belemnite which indicates mild alteration of samples.

In conclusion, both carbon and oxygen isotopic values of carbonate rock samples are much more negative than both isotopic of belemnite's standard values. The negative values of oxygen isotope are referred to as light which means a higher proportion of the light isotope ^{16}O (enriched in ^{16}O). In case of salinity changes (sea water mixes with fresh water), a negative values of $\delta^{18}\text{O}$ and $\delta^{13}\text{C}$ is expected, because the light isotopes ^{16}O and ^{12}C are more concentrated in fresh water than in sea water (Bartolini, 2003). Based on the carbon and oxygen isotopic analysis from Wyoming, the Lower Sundance Formation has been diagenetically altered by meteoric water since deposition during the Jurassic. As a result, carbon and oxygen isotopes can not be used to determine original sea water chemistry. However, isotopic composition values from the belemnite can be used to determine paleotemperature.

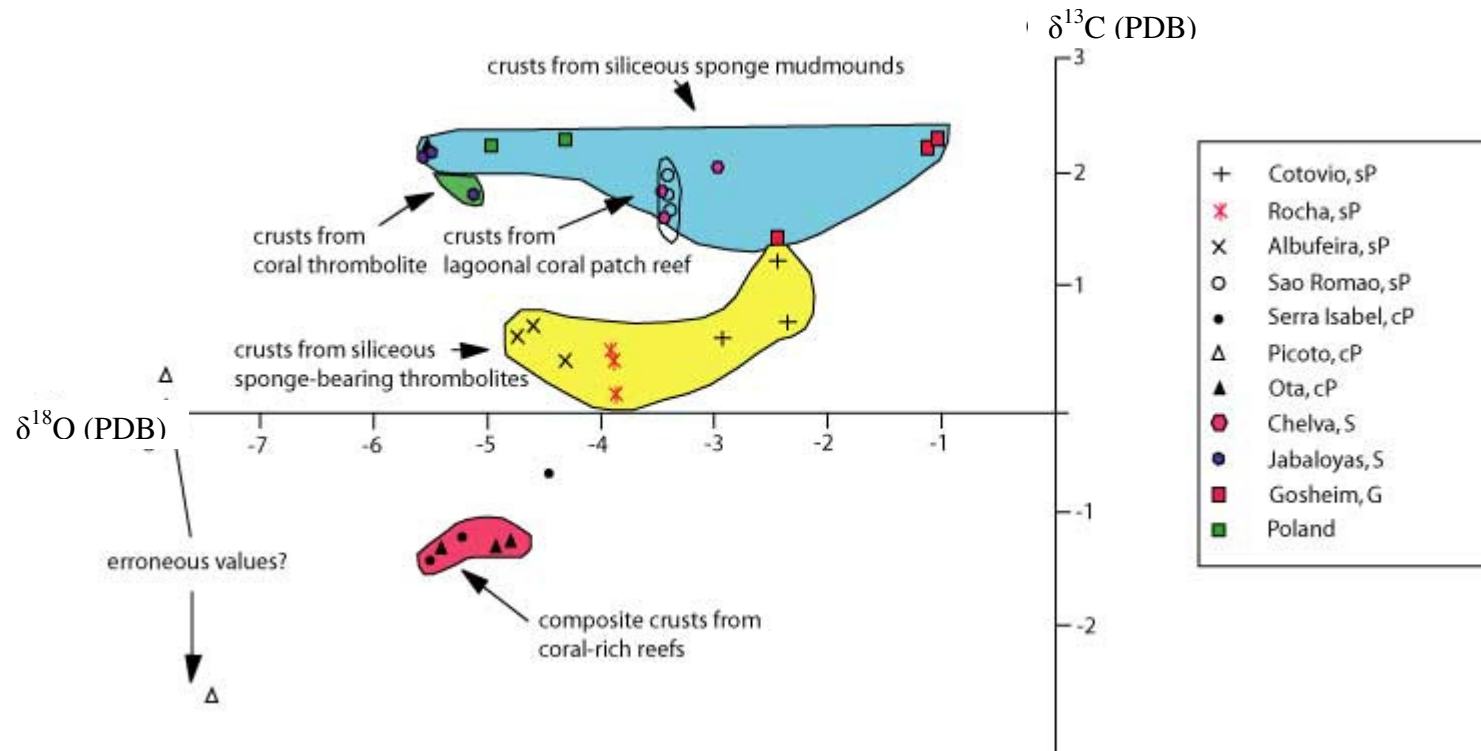


Figure 32: Carbon and oxygen isotope values for selected microbial crusts from Oxfordian and Kimmeridgian reefs.

sP: southern Portugal; cP: central Portugal; S: eastern Spain; Celtiberian ranges; G: southwestern Germany.

(From Leinfelder, 1993)

B. Climate Interpretation

Because of its stable shell composition, the isotopic values of the belemnites (table 4) were used to determine paleotemperature. Isotopes can be used to calculate paleotemperature according to the following equation (for low-magnesium calcite):

$$t(^{\circ}\text{C}) = 16.0 - 4.14(\delta_{\text{carbonate}} - \delta_{\text{water}}) + 0.13(\delta_{\text{c}} - \delta_{\text{w}})^2 \quad (\text{Parrish, 1998})$$

The paleotemperature of the Middle Jurassic (Late Bathonian to Early Callovian) seawater based on the belemnite samples from Wyoming is calculated to 15-17°C. Parrish (1998) suggested that the calculated temperature of belemnites were cooler than the actual sea- surface temperatures because belemnites probably recorded the temperatures of a mixture of surface and deeper water on the account of their movement to the water column. Dott and Batten, (1971) pointed to the evidence of warm Jurassic climate at mid-latitudes which was determined in 1951 as “O¹⁸:O¹⁶ ratios in Jurassic belemnoids from 57° North latitude (equivalent to Scotland or southern Alaska) points to an average annual sea water temperature of 14°-20°C (54°- 68°F), or roughly 15°C warmer than is typical at that latitude today”.

CHAPTER VII

CONCLUSIONS

The Middle Jurassic microbial buildups in Bighorn Basin of northern Wyoming were studied by field measurements, petrographic and isotopic analyses. The microbial thrombolites from the Lower Sundance Formation have a clotted characteristic with patchy feature in the field. The outcrop is composed of several thrombolites heads and these clotted features of thrombolites can easily see both under macroscopic scale and under microscopic scale. Based on the petrographic analyses of the Lower Sundance rocks at the study section provides more supporting information of the organisms for the climatic interpretation for the Middle Jurassic microbial thrombolite.

Cyanobacteria and segmented algae are the primary organisms that made up these microbial thrombolites. *Girvanella* is the most common type of cyanobacteria within the thrombolite units. Their tangled tubes tend to twist together to form nodules and encrust on any other particles or organisms. *Girvanella* have a clotted characteristic under the microscope. Other type of organisms includes *Cayeuxia* (Chlorophyta) and *Solenopora* (Rhodophyta) algae. Ostracods are abundant throughout the Lower Sundance section from wackestone at the bottom of section to microbial thrombolite at the top of the study section. In this study case, two genera of ostracods *Cytherella* (=Cytherelloidea?) and *Leptocythere* were identified in thin sections of packstones from the study area. The distribution of *Cytherella* (=Cytherelloidea?) has been interpreted as an indicator for relatively warm water temperatures (mean water temperature exceeds 10°C). Packstones that contain these ostracods are interpreted as originating in warm water marine environments.

Carbon and oxygen stable isotopic compositions have been studied for the entire stratigraphic section of the Lower Sundance Formation. The negative trend of both oxygen and carbon isotope (depletion of ¹⁸O and ¹³C) in the studied units can be explained by a meteoric alteration. The paleotemperature of the Middle Jurassic (Late Bathonian to Early Callovian) seawater based on the belemnite samples from Wyoming is calculated to about 15-17°C. As a result the paleoclimate setting of the Lower Sundance Formation can be interpreted as an arid to semi-arid environment.

REFERENCES

LIST OF REFERENCES

- Armstrong, H. A., and Brasier, M. D., *Microfossils*, Second Edition, Malden, MA, Blackwell Publishing Ltd, 2005.
- Attendorf, H.-G., and Bowen, R.N.C., *Radioactive and stable isotope geology*, First Edition, London, New York, Chapman & Hall, 1997.
- Bartolini, A., Pittet, B., and Mattioli, E., 2003, "Shallow-Platform Palaeoenvironmental Conditions Recorded in Deep-Shelf Sediments: C and O Stable Isotopes in Upper Jurassic Sections of Southern Germany (Oxfordian-Kimmeridgian)", *Sedimentary Geology*, Vol. 160, pp. 107-130.
- Bertling, M., and Insalaco, E., 1998, "Late Jurassic Coral/Microbial reefs from the Northern Paris Basin-facies, Palaeoecology and Palaeobiogeography", *Palaeogeography, Palaeoclimatology, Palaeoecology*, Vol. 139, pp. 139-175.
- Bissell, H. J., 1970, *Petrology and Petrography of Lower Triassic Marine Carbonates of Southern Nevada*, International sedimentary petrographical series, Vol. 14.
- Blackstone, D. L. Jr., 1971, *The Traveler's Guide to the Geology of Wyoming*, Bighorn Basin, pp.14
- Boggs, Sam, Jr., *Principles of Sedimentology and Stratigraphy*, Third Edition, Englewood Cliffs, N.J., Prentice Hall, 2001.
- Burne, R.V., and Moore, L.S., 1987, "Microbialites: Organosedimentary Deposits of Benthic Microbial Communities", *PALAIOS*, Vol. 2, pp. 241-254.
- Bullock, J. M., and Wilson, W. H., 1969, The Geological Survey of Wyoming, Gypsum Deposits in the Cody Area, Park County, Wyoming, Preliminary Report, No. 9, pp. 2-12.
- Cowen, R., 1988, "The Role of Algal Symbiosis in Reefs through Time", *PALAIOS*, Vol. 3, Reefs Issue, pp. 221-227.
- Deckker, P. D., Colin, J.P., and Peypouquet, J.P., *Ostracoda in the Earth Sciences*, New York, Elsevier, 1988.
- Dott, R. H., and Batten, R. L., *Evolution of the Earth*, New York, McGraw-Hill, 1971.
- Dupraz, C., and Strasser, A., 2002, "Nutritional Modes in Coral-Microbialite Reefs (Jurassic, Oxfordian, Switzerland): Evolution of Trophic Structure as a Response to Environmental Change", *PALAIOS*, Vol.17, pp. 449-471.
- Flugel, E., *Fossil Algae*, New York, Springer-Verlag, 1977.
- Foofes, E., Geneva, 1995, "Development and Eustatic Control of an Upper Jurassic Reef Complex (Saint Germain-de-Joux, Eastern France)", *Facies*, Vol. 33, pp. 129-150.
- Fürsich, F.T., Singh, I.B., and Joachimski, M., 2005, "Palaeoclimate Reconstructions of the Middle Jurassic of Kachchh (western India): an integrated approach based on palaeoecological, oxygen isotopic, and clay mineralogical data", *Palaeogeography, Palaeoclimatology, Palaeoecology*, Vol.217, pp. 289-309
- George, D. Stanley Jr., 1998, "The History of Early Mesozoic Reef Communities: A Three-Step Process", *PALAIOS* Vol. 3, Reef Issue, pp. 170-183.

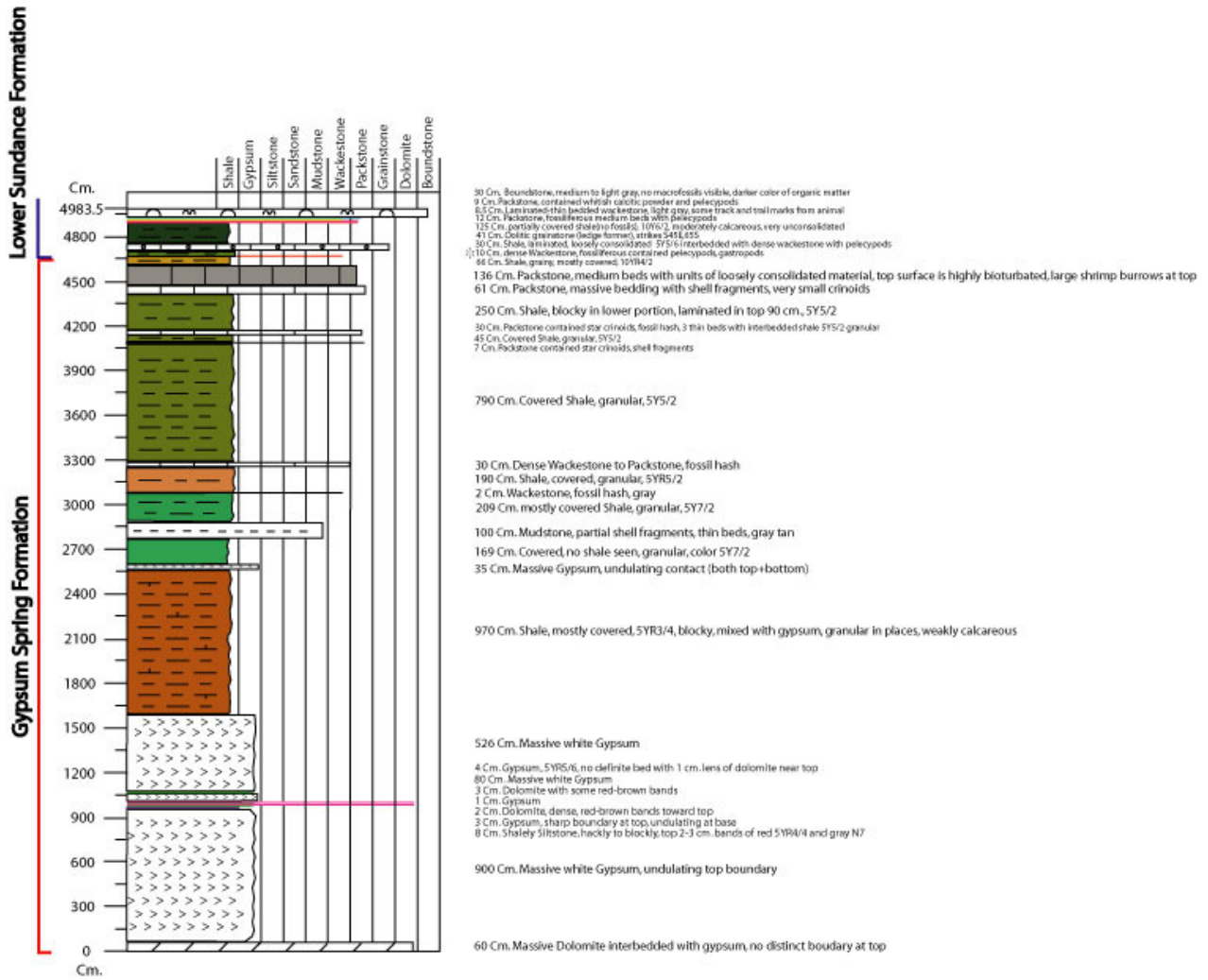
- Gomez-Perez, I., 2003, "An Early Jurassic Deep-Water Stromatolitic Bioherm Related Possible Methan Seepage (Los Molles Formation, Neuquen, Argentina)", *Palaeogeography, Palaeoclimatology, Palaeoecology*, Vol. 201, pp. 21-49.
- Grossman, E. L., Zhang, C., and Yancey, T.E., 1991, "Stable-isotope Stratigraphy of Brachiopods From Pennsylvanian Shales in Texas", *GSA Bulletin*, Vol. 103, pp. 953-965.
- Hallam, A., *Jurassic Environment*, New York, Cambridge University Press, 1975
- Halverson, G. H., *Highway Geology of Wyoming*, Wyoming Geological Association, 1964
- Hoefs, J., *Stable Isotope Geochemistry*, Fifth Edition, New York, Springer, 2004
- Horowitz, A. S., and Potter, P. E., *Introductory Petrography of Fossils*, New York, Springer-Verlag, 1971.
- Imlay, R. W., 1956, "Marine Jurassic Exposed in Bighorn Basin, Pryor Mountains, and Northern Bighorn Mountains, Wyoming and Montana", *AAPG Bulletin*, Vol. 40, No. 4, pp. 562-599.
- Imlay, R. W., 1980, "Jurassic Paleobiogeography of the Conterminous United States in Its Continental Setting", *Geological Survey Professional Paper 106*.
- Insalaco, E., and Birmingham, 1999, "Facies and Palaeoecology of Upper Jurassic (Middle Oxfordian) Coral Reefs in England", *Facies*, Vol. 40, pp. 81-100.
- Johnson, E. A., 1991, "Depositional History of Jurassic Rocks in the Area of the Powder River Basin, Northeastern Wyoming and Southeastern Montana", *U.S.G.S. Bulletin*, 1917-J, pp. J1-J37.
- Johnson, J. Harlan, *Limestone-Building Algae and Algal Limestones*, Golden, Colorado School of Mines, Dept. of Publications, 1961.
- Kennard, J.M., and James, N.P., 1986, "Thrombolites and Stromatolites: Two Distinct Types of Microbial Structures", *PALAIOS*, Vol.1, pp. 492-503.
- Kocurek, G., and Dott, R. H., Jr., 1983, "Jurassic Paleogeography and Paleoclimate of the Central And Southern Rocky Mountains Region, Mesozoic Paleogeography of West-Central United States", *S.E.P.M.*, Rocky Mountain Section, pp. 101-116.
- Lehmann, P. J., and Greenlee, S. M., *Carbonate Sequence Stratigraphy: Recent Developments and Applications*, AAPG Memoir 57, Tulsa, OK, AAPG, 1993.
- Leinfelder, R. Reinhold, and Nose M., 1993, "Microbial Crusts of the Late Jurassic: Composition, Palaeoecological Significance and Importance in Reef Construction", *Facies*, Vol. 29, pp. 195-230.
- Leinfelder, R., Krautter, M., Reinhold, and Nose, M., 1994, "The Origin of Jurassic Reefs: Current Research Developments and Results", *Facies*, Vol. 31, pp. 1-56.
- Leinfelder, R. Reinhold, Schmid, D. U., Nose, M., and Werner, W., 2002, "Jurassic Reef Patterns-The Expression of a Changing Globe, Phanerozoic Reef Patterns", *SEPM Special Publication*, No. 72, pp. 465-520.
- Levin, H. L., *Ancient Invertebrates and Their Living Relatives*, Upper Saddle River, NJ, Prentice-Hall Inc, 1999.

- Levorsen, A.I., *Geology of Petroleum*, Second Edition, San Francisco, CA, W.H. Freeman and Company, 1967.
- Lo Forte, G.L., Orff, F., and Rossell, L., 2005, "Isotopic Characterization of Jurassic Evaporites, Aconcague-Neuquén Basin, Argentina", *Geologica Acta*, Vol. 3, pp. 155-161.
- Love, J. D., *Geology along the Southern Margin of the Absaroka Range*, Baltimore, MD, Waverly Press, Inc., 1939.
- Mette, W., 1997, "Palaeoecology and Palaeobiogeography of the Middle Jurassic Ostracods of Southern Tunisia", *Palaeogeography, Palaeoclimatology, Palaeoecology*, Vol. 131, pp. 65-111.
- Miall, D. A., *The Geology of Stratigraphic Sequences*, Germany, Springer-Verlag Berlin Heidelberg, 1997,
- Moore, R. C., *Treatise on Invertebrate Paleontology*, New York, Geological Society of America, University of Kansas Press, 1961
- Morettini, E., Santantonio, M., and Bartolini, A., 2002, "Carbon Isotope Stratigraphy and Carbonate Production during the Early-Middle Jurassic: Examples from the Umbria-Marche-Sabina Apennines (Central Italy)", *Palaeogeography, Palaeoclimatology, Palaeoecology*, Vol. 184, pp. 251-273.
- Mills, N. K., *Wyoming Stratigraphy*, Wyoming, Wyoming Geological Association, 1956.
- Oliver, N., and Leinfelder, R. R., 2003, "Microbialite Morphology, Structure and Growth: A Model of the Upper Jurassic Reefs of the Chay Peninsula (Western France)", *Palaeogeography, Palaeoclimatology, Palaeoecology*, Vol. 193, pp. 383-404.
- Olivier, N., and Carpenter, C., 2004, "Coral-Microbialite Reefs in Pure Carbonate versus Mixed Carbonate-Siliciclastic Depositional Environments: The Example of the Pagny-sur-Meuse Section (Upper Jurassic, Northeastern France)", *Facies*, Vol. 50, pp. 229-255.
- Parcell, C. W., and Leinfelder, R. R., Mancini, E. A., 2004, Upper Jurassic thrombolite reservoir play, northeastern Gulf of Mexico, *AAPG Bulletin*, V. 88, No. 11, pp. 1573-1602
- Parrish, J. T., *Interpreting Pre-Quaternary Climate from the Geologic Record, Introduction*, New York, Columbia University Press, 1998.
- Peterson, J. A., 1957, "Marine Jurassic of Northern Rocky Mountains and Williston Basin", *AAPG Bulletin*, Vol. 41, No. 3, pp. 399-440.
- Pratt, B. R., 1984, "Epiphyton and Renalcis-Diagenetic Microfossils from Calcification of Coccoid Blue-Green Algae", *Journal of Sedimentary Petrology*, Vol. 54, No. 3, pp. 948-971.
- Rankama, K., *Isotope Geology*, New York, McGraw-Hill, 1954.
- Ripperdan, R.L., 2001, Stratigraphic "Variation in Marine Carbonate Carbon Isotope Ratios", *Stable Isotope Geochemistry; Reviews in Mineralogy & Geochemistry*, Vol. 43, pp. 637-659.
- Rosales, I., Robles, S., and Quesada, S., 2005, "Oxygen Isotope, Mg/Ca and Sr/Ca records of Lower Jurassic Belemnite Shells: Implications for the Interpretation of the Isotopic record of old fossils and Changes of Ancient Seawater Paleotemperature", *Geophysical Research Abstracts*, Vol.7, 09355

- Samuelson, A. C., 1974, Introduction to the Geology of the Bighorn Basin and Adjacent Areas, Wyoming and Montana.
- Schmitt, M., and Monninger, W., 1977, Fossils Algae, Stromatolites and Thrombolites in Precambrian/Cambrian Boundary Beds of the Anti-Atlas, Morocco: Preliminary Results, p. 80-85.
- Scholle, P. A., 1978, Carbonate Rock Constituents, Textures, Cements, and Porosities: AAPG Memoir 27.
- Scholle, P. A., and Arthur, M. A., 1980, Carbon Isotope Fluctuations in Cretaceous Pelagic Limestones: Potential Stratigraphic and Petroleum Exploration Tool, AAPG Bulletin, Vol. 64, No. 1, pp. 67-87.
- Schopf, J. W., *Cradle of Life*, Princeton, NJ, Princeton University Press, 1999.
- _____. *Earth's Earliest Biosphere: Its origin and Evolution*, Princeton, NJ, Princeton University Press, 1983.
- Schudack, M.E., 1999, "Ostracoda (marine/nonmarine) and palaeoclimate History in the Upper Jurassic of Central Europe and North America", *Marine Micropaleontology*, Vol. 37, pp. 273-288.
- Schumude, D. E., 2000, "Interplay of Paleostucture, Sedimentation and Preservation of Middle Jurassic Rocks, Bighorn Basin, Wyoming", *The Mountain Geologist*, Vol. 37, No. 4, pp.145-155.
- Scott, R. W., 1988, "Evolution of Late Jurassic and Early Cretaceous Reef Biotas", *PALAIOS*, Vol. 3, Reefs Issue, pp. 184-193.
- Shinn, E. A., *Carbonate Depositional Environments*, Tulsa, OK, The American Association of Petroleum Geologists, 1983.
- Spearing, D. R., Lageson, D. R., *Roadside Geology of Wyoming*, Missoula, MT, Mountain Press Publishing Company, 1988.
- Toomey, D. F., Nitecki, M. H., Riding, R., and Voronova, L., *Paleoalgology*, Germany, Springer-Verlag Berlin Heidelberg, 1985.
- Walter, M. R., *Stromatolites*, New York, Elsevier, 1976.
- Wicander, R., and Monroe, J., S., *Historical Geology*, Fourth Edition, Canana, Thomson Learning, Inc., 2004.
- Wray, J. L., *Calcareous Algae*, New York, Elsevier Scientific Publishing Company, 1977.
- Ziegler, V., 1917, "The Oregon Basin Gas and Oil Field: Park County", *Wyoming Geological Survey Bulletin*, No. 15, pp. 209-242.

APPENDICES

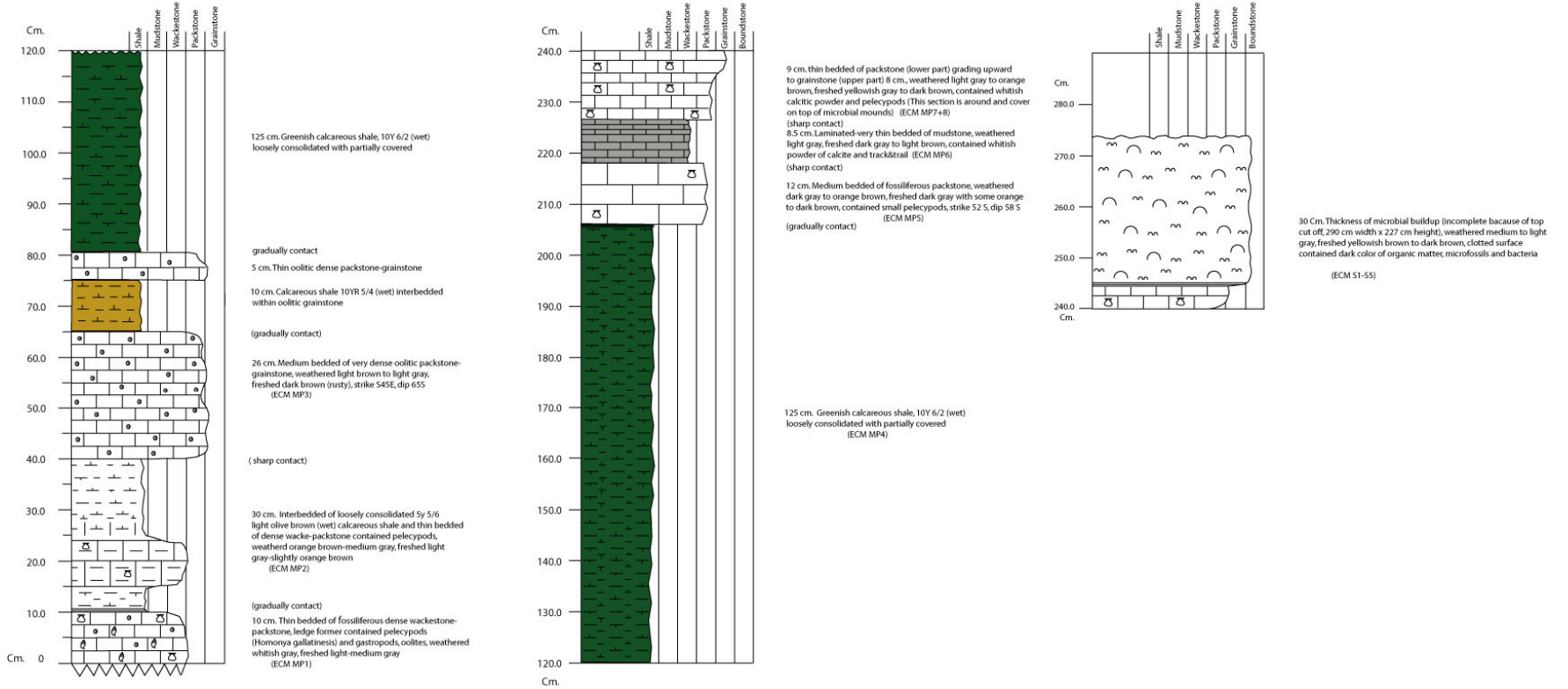
Appendix A: Stratigraphy of Gypsum Spring and Lower Sundance Formation



Stratigraphic section of Middle Jurassic (Gypsum Spring and Lower Sundance Formation)

at east of Cedar Mountain

Stratigraphy of Lower Sundance Formation in the study area at east of Cedar Mountain outcrop, WY



Stratigraphic section of Middle Jurassic (Lower Sundance Formation) at east of Cedar Mountain

Appendix B: Hand Sample and Thin Section Description

Table 3: Hand Samples Description

East of Cedar Mountain 14-T52N-R102W, south of Cody, Wyoming; S52E, dip 58SW

Note: rain previous day; samples were slightly wet

Description	Sample #	Thickness (cm)	Cumulative Thickness (cm)
Lower Sundance Formation			
1) Thrombolite/microbial buildups, clotted surface and contain several heads, medium to light gray weathered color, yellowish brown to dark brown freshed color, with crystalline-microcrystalline texture, composed of dark color of organic matter, microfossils, and bacteria	ECM S1-S5	30	30
2) Medium gray mudstone (substrate underneath the microbial mounds), medium to fine grained crystalline texture, contained small burrows	ECM MP9		
3) Thin bedded of mudstone to wackestone, yellowish gray to light brown weathered, dark brown freshed color, coarse-medium grained texture, contain lots of microfossils and pelecypods	ECM MP8	8	38
4) Thin bedded of packstone, slightly ledge former and partly cover up/overlap on top of the mounds, medium gray to orange brown in weathered color, dark brown with some yellowish freshed color, medium to very fine grained crystalline texture, react with acid, contain slightly powder of calcite, composed of shell fragments, pelecypods	ECM MP7	9	47
5) Laminated to very thin bedded of mudstone, weathered and freshed medium gray to brown, medium to fine grained crystalline texture, contained whitish powder of calcite and track&trail (sharp contact with overlying and underlying beds)	ECM MP6	8.5	55.5
6) Medium bedded of fossiliferous sandy packstone, weathered dark gray to orange brown, freshed dark gray with some orange to dark brown, medium to fine grained sandy with crystalline texture carbonate, contained small pelecypods, strike 52 E, dip 58 due S	ECM MP5	12	67.5
7) Greenish colored shale, 10Y 6/2 (wet), blockly, loosely consolidated with partially covered, fine grained with crystalline texture, gradually to overlying bed	ECM MP4	125	192.5

8) 5 cm of thin oolitic very dense packstone to grainstone on the upper part interbedded with 10 cm of calcareous shale 10 YR 5/4 (wet) that gradually with underlying bed 26 cm of medium bedded of oolitic grainstone, weathered light brown to light gray, freshed dark brown (rusty), strike S45E, dip 65 due S

ECM MP3 41 233.5

9) Interbedded of loosely consolidated 5Y 5/6 light olive brown (wet) calcareous shale and thin bedded of dense wackestone to packstone with crystalline texture, contained pelecypods, weathered orange brown to medium gray, freshed light gray to orange brown (sharp contact with overlying beds)

ECM MP2 30 263.5

10) Thin bedded of fossiliferous dense wackestone to packstone, ledge former with bumpy surface contained pelecypods (*Homonya gallatinesis*) and gastropods, oolites and small circular depressions, weathered whitish gray, freshed light to medium gray, crystalline texture

ECM MP1 10 273.5

Total thickness of Lower Sundance Formation

273.5 273.5

Gypsum Spring Formation

11) Silty shale, mostly covered, 10YR 4/2

66 339.5

12) Medium bedded of packstone with unit of loosely consolidated material, same fossil assemblage throughout, top surface is highly bioturbated, large shrimp burrows at top

AM 10 136 475.5

13) packstone contained pelecypod's shell fragments and very small crinoids with crystalline texture

AM 9 61 536.5

14) Silty shale, very fine to silt grained size, blocky in lower portion, laminated in top 90 cm (includes limestone and gypsum stringers)

AM 8 250 786.5

15) 3 thin bedded of packstone interbedded with granular shale 5Y 5/2, crystalline texture, contained abundant of fossils such as star crinoids, pelecypods shells

AM 7 30 816.5

16) Covered shale, granular 5Y 5/2

45 861.5

17) 2 bedded of packstone (lower 2 cm, upper 5 cm), contained star crinoids, shell fragments

7 868.5

18) Covered shale, granular 5Y 5/2

790 1658.5

19) Thin bedded of dense wackestone to packstone, crystalline texture, abundant of fossils such as pelecypods shells(<0.5 cm in size)	AM 6	30	1688.5
20) Covered shale, granular 5Y 5/2		190	1878.5
21) wackestone, gray color, fossil hash		2	1880.5
22) Mostly covered shale, granular 5Y 7/2		209	2089.5
23) Thin bedded of sandy mudstone, gray tan color, highly calcareous, medium to fine grained sand with crystalline texture, contained partial shell fragments	AM 5	100	2189.5
24) Covered, no shale seen, 5Y 7/2, possibly modern color		169	2358.5
25) Massive gypsum, undulating contacts (both top and bottom)		35	2393.5
26) Shale (mostly covered), 5YR 3/4, blocky, mixed with gypsum, granular in places, hard to see bedding, weakly calcareous		970	3363.5
Note: all of the above section was measured after laterally moved			
27) Massive white gypsum (top of gypsum)		526	3889.5
28) Thin bedded of gypsum 5YR 5/6 with no definite bed and 1 cm thick lens of dolomite (N7) near top		4	3893.5
29) Massive white gypsum		80	3973.5
30) Dolomite N7 with some red-brown bands		3	3976.5
31) Gypsum		1	3977.5
32) Dense dolomite N7, crystalline texture, red-brown bands toward top	AM 4	2	3979.5
33) Gypsum, sharp boundary at top, undulating at base		3	3982.5
34) Shaly siltstone, hackly to blockly, fine to silt grained size, red bands 5YR 4/4 and gray bands N7 at the top of 2-3 cm	AM 3	8	3990.5
35) Massive white gypsum with crystalline texture	AM 2	900	4890.5
36) Massive dolomite N7 interbedded with gypsum and no distinct boundary at top, dolomite have crystalline to fine grained size	AM 1	60	4950.5
Total thickness of Gypsum Spring Formation		4677	

Table 4: Petrographic Analysis

Thin section descriptions from east of Cedar Mountain, 14-T52N-R102W, south of Cody, Wyoming; S52E, dip 58SW

All thin sections were dyed in alizarin to detect calcite mineral.

Sample #	Type of Rock	Allochem	Matrix	Mineralogy	Type of Organisms
ECM MP1	Packstone	1) Ooids, 2) peloids, 3) skeletal grains such as ostracods > 30% with some pelecypods and foram, and 4) other microorganisms such as Rhodophyta and Chlorophyta algae	Micrite	Calcite	Ostracods (<i>Cytherella sp.</i> , <i>Leptocythere sp.</i>), foram, pelecypods such as <i>Homonya sp.</i> , algae: <i>Solenopora (Rhodophyta)</i> and <i>Cayeuxia</i>
ECM MP2	Packstone	1) Skeletal grains of gastropods, ostracods and pelecypods, 2) peloids with some ooids, 3) intraclasts with long rectangular shape (~1mm long), and 4) algae	Micrite with some sparry calcite	Calcite	Bryozoan fragments, segmented algae, ostracods (<i>Leptocythere sp.</i>)
ECM MP3	Grainstone	1) Ooids > 50%; both in circular and elongate shape with sub-rounded to rounded, 2) some skeletal grains and 3) algae	Sparry calcite	Calcite	bryozoan fragments and algae: <i>Solenopora</i> , cyanobacteria: <i>Girvanella</i>
ECM MP5	Sandy dense wackestone to packstone	1) Skeletal grains >10%, 2) ooids, 3) intraclasts, some contain shell fragments inside, 4) pellets/peloids mostly sub-angular, 5) quartz sand	Micrite with small burrows (bioturbated matrix)	Calcite, quartz	Pelecypods and ostracods

Sample #	Type of Rock	Allochem	Matrix	Mineralogy	Type of Organisms
ECM MP6	Mudstone	1) Skeletal grains of ostracods, 2) peloids and 3) <i>Girvanella</i>	Micrite with several fractures indicates highly weathering	Calcite	Ostracod shell fragments, Cyanobacteria: <i>Girvanella</i>
ECM MP7	Dense wackestone to packstone	1) Skeletal grains	Micrite and sparry calcite with iron oxide/pyrite (reducing condition)	Calcite, pyrite, and iron oxide	Foraminifera, ostracods (<i>Cytherella sp.</i>)
ECM MP8	Mudstone	1) skeletal grains ~ 8%, some scattered some pack together	Micrite > sparry calcite with some iron oxide and lots of fractures	Calcite, and iron oxide	Highly content of ostracods
ECM MP9	Mudstone	1) Skeletal grains ~ 3-5%, 2) peloids 3) clotted-looking algae	Micrite with some sparry calcite	Calcite	Algae, foraminifera, ostracods (<i>Leptocythere sp.</i>), clotted-looking of <i>Girvanella</i>
ECM S1	Bindstone/Thrombolite	Highly clotted-looking of rock that formed by encrusting or binding of organisms such as algae and microorganisms and also composed of numerous fractures	Micrite, with sparry calcite inside the organisms	Calcite	Algae with elongate shape and divided by chamber-like or septa and <i>Girvanella</i>
ECM S2	Bindstone/Thrombolite	Skeletal grains and also clotted-looking algae and microorganisms	Mostly micrite matrix with some sparry calcite	Calcite, and iron oxide	Algae with elongate shape and contained septa, larger size than S1 sample and <i>Girvanella</i> , some ostracods

Sample #	Type of Rock	Allochem	Matrix	Mineralogy	Type of Organisms
ECM S3	Bindstone/ Thrombolite	Highly clotted-looking algae, contain lots of algae and also lots of fractures	Micrite	Calcite	Algae with elongate shape and contained septa with sediment fill inside and x-talline structure and <i>Girvanella</i>
ECM S4	Bindstone/ Thrombolite	Algae and microorganisms, not many fractures as S3, and coated grains	Micrite	Calcite, and iron oxide	Algae with elongate shape and divided by chamber-like or septa and <i>Girvanella</i>
ECM S5	Bindstone/ Thrombolite	Highly clotted-looking <i>Girvanella</i> , contain higher segmented algae than others	Micrite	Calcite, and iron oxide, and black vein of mineral?	Algae with elongate shape and contained septa with sediment fill inside and x-talline structure and small amount of <i>Girvanella</i>

Appendix C: Algae and Cyanobacteria Index

Classification and Description of Algae and Cyanobacteria

Phylum: RHODOPHYCOPHYTA (Red Algae)

Class: RHODOPHYCEAE

Order: CRYPTONEMIALES

Family: SOLEONOPORACEAE

Genus: SOLENOPORA

1) *Solenopora* sp. from sample ECM MP1

The classification of the algae from Phylum to Genus is following Johnson (1961). According to Riding (1985), this genus are classified by their morphology which belong to tubiform with fan-like or radiating branched masses of tube. The most apparent structures in vertical sections are the vertical or slightly radiating cell threads (Johnson, 1961). The characteristic growth forms of this genus are rounded, nodular masses (Wray, 1977). In transverse section, cells are rounded to polygonal, averaging 30-50 microns in diameter (Wray, 1977). Generic range: Cambrian to Cretaceous (Johnson, 1961). Geographic distribution: Nearly worldwide (Johnson, 1961).

Phylum: CHOLOROPHYCOPHYTA (Johnson, 1961), CYANOPHYTA (Wray, 1977)

Class: CHLOROPHYCEAE

Order: SIPHONALES

Family: CODIACEAE

Genus: CAYEUXIA

1) *Cayeuxia* from sample ECM MP1

Plants form rounded tufts or cushions, ranging in diameter from a few millimeters to more than a centimeter. The tufts consist of a mass of loosely-packed, radially-arranged, branching tubular filaments. The type of branching characterizes the genus: the original filament continues straight with branch starting off at an angle of nearly 45° for a short distance (Johnson, 1961). Generic range: Jurassic and Lower Cretaceous (Johnson, 1961).

Phylum: SCHIZOPHYTA (Johnson, 1961), CYAOBACTERIA (CYANOPHYTA) (Wray, 1977)

Family: Belong to several family (Wray, 1977)

Genus: GIRVANELLA

1) *Girvanella* from sample ECM MP 3, MP9, and ECM S1 to S5

This genus is characterized by flexuous, tubular filaments of uniform diameter (Johnson, 1961 and Wray, 1977), composed of relatively thin micritic wall (Riding, 1985). Frequently, the tubes develop around a nucleus and form small rounded or bean-shaped masses (Johnson, 1961). Filaments form loosely and usually occur in groups, twisted together to form nodules and encrusting masses on various objects (Wray, 1977). Generic range: Cambrian to Cretaceous (Johnson, 1961). Geographic distribution: worldwide (Johnson, 1961).